Polyhedron

Triazacyclohexane Chromium Triflate Complexes as Precursors for the Catalytic Selective Olefin Trimerisation and its Investigation by Mass Spectrometry

--Manuscript Draft--

Manuscript Number:	POLYH-D-19-01297R3
Article Type:	VSI: John Bercaw
Keywords:	Catalysis Coordination Chemistry Selective Olefin Trimerisation Chromium Electrospray Mass Spectrometry
Corresponding Author:	Randolf D Köhn, Ph. D. University of Bath, Bath, UNITED KINGDOM
First Author:	Randolf D Köhn, Ph. D.
Order of Authors:	Randolf D Köhn, Ph. D.
	Alexander G. N. Coxon, Ph.D.
	Samaphon Chunawat, MSc
	Callum Heron
	Shahram Mihan, Dr
	Catherine L. Lyall
	Shaun Reeksting
	Gabriele Kociok-Köhn, Dr
Manuscript Region of Origin:	UNITED KINGDOM
Abstract:	A novel set of linear α-olefin trimerisation pre-catalysts is presented. The R 3 TACCr(OTf) 3 (R 3 TAC = 1,3,5-trialkyl-1,3,5-triazacyclohexane) complexes produce an active system after facile activation with less than 10 equivalents of trialkylaluminium. Isomerisation was observed in many cases, which is proposed to occur via the π-allyl complex mechanism, though this was minimised by optimisation of the reaction conditions. The pre-catalysts can be synthesised from R 3 TACCrCl 3 in neat TfOH or by addition of R 3 TAC to Cr(OTf) 3 or better Cr(OTf) 3 (THF) 3 , the synthesis and structure of which is presented here. The use of this highly defined system allowed the identification of 2-methyl-1-hexene as a side product of activation with AlMe 3 , in agreement with the proposed metallacyclic mechanism. Isomer distribution of the trimer product is similar to R 3 TACCrCl 3 /MAO activated systems and depends mostly on the ligand substituent R. ESI mass spectrometry of an ortho -difluorobenzene solution of the activated catalyst was analysed at different stages of reaction. A series of signals was observed that matched those expected for cationic chromium species predicted by the metallacyclic mechanism. In particular, [R 3 TACCrMe 2] + was observed to form immediately after alkylation with AlMe 3 , while [R 3 TACCr(olefin) n] + (n = 0,1,2,3,4 and olefin= 1-hexene or 1-octene) formed after addition of 1-hexene. Absence of any detected tetramer and observation of [R 3 TACCr(olefin) 4] + leads to the conclusion that a metallacycloheptane-olefin complex may lead to β-H abstraction rather than insertion and may even be required to avoid formation of [R 3 TACCr(olefin) 1] + which is observed in only very small amounts indicating a low stability. Chromium(I) complexes [R 3 TACCr(arene)] + with the arene solvent can also be observed and their signal intensity indicate a relative stability of o-C 6 H 4 F 2 < cymene < benzene < PhF, toluene < p-xylene.
Response to Reviewers:	Reviewer #1: The term “reductive elimination” was changed to “-H abstraction” and the direct route transition state added to Scheme 2.

Dr. Randolf D. Köhn
Department of Chemistry
University of Bath
Claverton Down
Bath, BA2 7AY
United Kingdom
Phone: (0044 1225) 38 3305
FAX: (0044 1225) 386 231
e-mail: r.d.kohn@bath.ac.uk
https://researchportal.bath.ac.uk/en/persons/randolf-kohn/

Gerard Parkin,
Department of Chemistry (Box 3115),
Columbia University,
3000 Broadway,
New York, New York 10027, USA.
email: parkin@columbia.edu
Tel. (212) 854-8247
Fax. (212) 932-1289

Bath, 17 April 2020

Dear Ged,

As discussed via email I have changed the term “reductive elimination” to “β-H abstraction” and added the direct route transition state to Scheme 2.

Best Regards

Randolf Köhn

Response to comments:

Reviewer #1:
The term “reductive elimination” was changed to “β-H abstraction” and the direct route transition state added to Scheme 2.

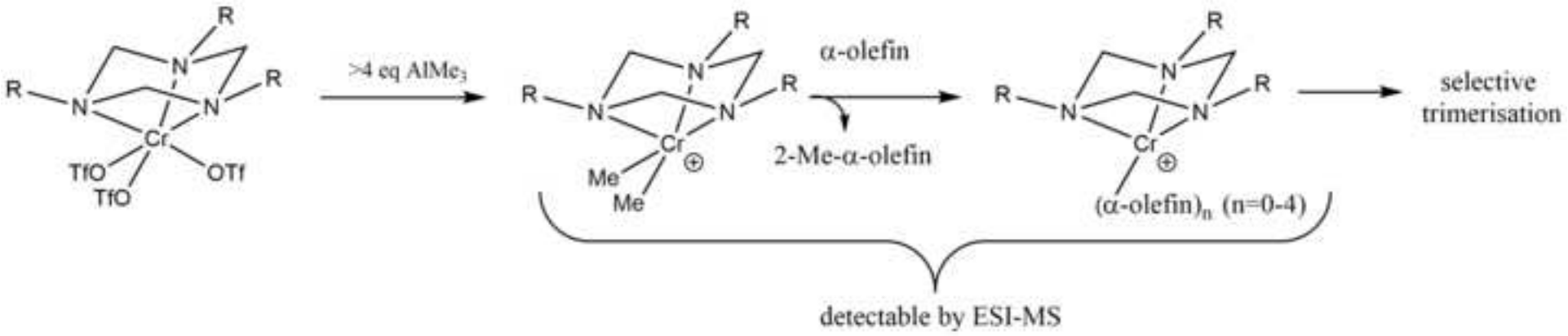

Graphical Abstract

A new type of triazacyclohexane (R_3TAC, L) complexes of $Cr(OTf)_3$ (OTf = trifluoromethanesulphonate) has been prepared from the corresponding chloride complexes in triflic acid or ligand addition to a new precursor $[Cr(OTf)_3(THF)_3]$. The new complexes require only four equivalents of AlR_3 to become active catalysts for the selective trimerisation of α-olefins and allow a study via ESI-MS during catalysis with observation of cations corresponding to the mass of $[LCrMe_2]^+$ as initial activation product, $[LCr(olefin)_n]^+$ (n=0-4) as members of the metallacyclic mechanism and [LCr(arene solvent)]$^+$ as intermediates proving the accessibility of Cr(I).

Triazacyclohexane Chromium Triflate Complexes as Precursors for the Catalytic Selective Olefin Trimerisation and its Investigation by Mass Spectrometry

Randolf D. Köhn*[a], Alexander G. N. Coxon[a], Samaphon Chunawat[a], Callum Heron[b], Shahram Mihan[c], Catherine L. Lyall[d], Shaun Reeksting[d], Gabriele Kociok-Köhn[d]

[a]Department of Chemistry, University of Bath, Claverton Down, Bath, BA2 7AY, UK

[b]Centre for Sustainable Chemical Technologies, University of Bath, Claverton Down, Bath, BA2 7AY, UK

[c]LyondellBasell, Basell Polyolefine GmbH, Industriepark Höchst, 65929, Frankfurt am Main, GERMANY

[d]Materials and Chemical Characterisation Facility (MC^2), University of Bath, Claverton Down, Bath, BA2 7AY, UK. https://doi.org/10.15125/mx6j-3r54

Dedicated to Prof. John Bercaw on the occasion of his 75th birthday.

*Corresponding author. Tel.: +44 1225 383305
E-mail address: r.d.kohn@bath.ac.uk

ABSTRACT

A novel set of linear α-olefin trimerisation pre-catalysts is presented. The $R_3TACCr(OTf)_3$ (R_3TAC = 1,3,5-trialkyl-1,3,5-triazacyclohexane) complexes produce an active system after facile activation with less than 10 equivalents of trialkylaluminium. Isomerisation was observed in many cases, which is proposed to occur *via* the π-allyl complex mechanism, though this was minimised by optimisation of the reaction conditions. The pre-catalysts can be synthesised from $R_3TACCrCl_3$ in neat TfOH or by addition of R_3TAC to $Cr(OTf)_3$ or better $Cr(OTf)_3(THF)_3$, the synthesis and structure of which is presented here. The use of this highly defined system allowed the identification of 2-methyl-1-hexene as a side product of activation with $AlMe_3$, in agreement with the proposed metallacyclic mechanism. Isomer distribution of the trimer product is similar to $R_3TACCrCl_3$/MAO activated systems and depends mostly on the ligand substituent R. ESI mass spectrometry of an *ortho*-difluorobenzene solution of the activated catalyst was analysed at different stages of reaction. A series of signals was observed that matched those expected for cationic chromium species predicted by the metallacyclic mechanism. In particular, $[R_3TACCrMe_2]^+$ was observed to form immediately after alkylation with $AlMe_3$, while $[R_3TACCr(olefin)_n]^+$ (n = 0,1,2,3,4 and olefin= 1-hexene or 1-octene) formed after addition of 1-hexene. Absence of any detected tetramer and observation of $[R_3TACCr(olefin)_4]^+$ leads to the conclusion that a metallacycloheptane-olefin complex may lead to β-H abstraction rather than insertion and may even be required to avoid formation of $[R_3TACCr(olefin)_1]^+$ which is observed in only very small amounts indicating a low stability. Chromium(I) complexes $[R_3TACCr(arene)]^+$ with the arene solvent can also be observed and their signal intensity indicate a relative stability of o-$C_6H_4F_2$ < cymene < benzene < PhF, toluene < p-xylene.

1. Introduction

The selective oligomerisation of ethylene, especially tri- and tetramerisation, has become an essential synthetic step in the production of widely used co-polymers such as Linear Low Density Polyethylene (LLDPE). The adoption of these processes has been driven by strong growth in demand for 1-hexene and 1-octene for use as co-monomers. These selective reactions are more expensive than traditional non-selective oligomerisation routes, such as the 'Aufbau' reaction, due to the use of more complex catalyst systems. Since commercialisation of the poorly defined Phillips Trimerisation Catalyst considerable research has focused on the preparation of well-defined pre-catalysts capable of similar efficiencies. [1,2]

Significant progress in recent years has led to the discovery of several systems that are competitive with the commercialised catalyst in terms of selectivity and activity. We have introduced very active triazacyclohexane based chromium complexes as pre-catalysts for the polymerisation and selective trimerisation of ethylene.[3,4] However, these systems are reliant on highly expensive trimethylaluminium derived activating agents such as various forms of methylaluminoxane (MAO or dried modified MAO, DMMAO), which severely reduces their economic viability. The activating agent typically accounts for a significant proportion of overall production costs due to the large excess required, typically 300-10,000 equivalents relative to the pre-catalyst. In order to find a true competitor to the Phillips system, which is activated with Et_2AlCl, a novel activation process is desirable in which the costly use of MAO variants is avoided.
In an attempt to overcome this barrier to commercialisation, increasing research is being performed into alternative activation methods. Most notably, Bercaw *et al.* recently described a two-step activation procedure for the highly active $(FI)TiCl_3$ ethylene trimerisation catalyst that avoids the need for MAO.[5] Wass *et al*. explored a different two-step approach, in which the pre-catalyst was oxidised in order to form the cation prior to alkylation, again avoiding the use of MAO.[6] We have been able to activate $R_3TACCrCl_3$ also with $[PhNMe_2H]$ $[B(C_6F_5)_4]/Al^iBu_3$.[7] In all cases two distinct activation steps were required in order to achieve activation, which would in turn result in considerable increases in production costs. To be truly viable, modification of the activation procedure should not result in additional synthetic steps and should require only a minimal excess of activating agent while avoiding MAO based species.
While there is extensive literature on selective ethylene trimerisation [1,2] only two systems capable of selective trimerisation of α-olefins have been described, a titanium based system by Bercaw et al. [5,8] and our triazacyclohexane chromium systems [9,10].
When undertaking a mechanistic investigation into catalytic systems a key challenge is the characterisation of intermediates within the catalytic cycle. This has proved to be the case for selective α-olefin trimerisation in just the same way as it has for numerous other systems. The metallacyclic mechanism originally proposed by Manyik [11] and Briggs [12] for this process has been supported by numerous experiments that have looked at different aspects of the reaction. For example, the strongest evidence to date was presented by Bercaw *et al*. who ruled out a chain growth mechanism with the use of a deuterium scrambling experiment.[13]

In contrast, direct observation of the proposed intermediates has seldom been reported due to the inherent difficulties associated with characterisation of such short-lived species. In 2009, the first NMR derived evidence for the existence of the proposed intermediates was presented for a tantalum based system.[14] However, tantalum systems demonstrate very low trimerisation activities in comparison to chromium based systems, which are therefore of more interest but cannot be investigated in the same manner due to their paramagnetic nature. For this reason, only limited spectroscopic analysis of chromium-based intermediates has been possible to date. In 1997 a chromacyclopentane species was synthesised directly by Jolly *et al*. [15] and successfully crystallised, confirming the proposed intermediates are viable but under very different conditions to α-olefin trimerisation. More recently, Bercaw *et al*. conducted an extensive UV-Vis and EPR spectroscopy investigation into ethylene trimerisation.[16] The results strongly support the proposed alkylation of the pre-catalyst during activation and provide considerable information on the oxidation state of the chromium species present.
Despite these advances, direct observation of chromacyclic and other proposed intermediates has remained elusive. One method for the identification of such species that has, until now, remained

unexplored is the use of electrospray mass spectrometry (ESIMS) although it has been successfully applied for other catalytic systems [17] and is even used to analyse MAO solutions[18]. This technique is a prime candidate for investigation of α-olefin trimerisation because the active intermediates are known to be cationic and are therefore readily detectible under the right conditions.

We describe herein an investigation into the substitution of chloride ligands, almost universally used in defined trimerisation pre-catalysts, with triflate anions to produce $R_3TACCr(OTf)_3$ species. The activation pathways available to these pre-catalysts were then explored in relation to the trimerisation of linear α-olefins. Many of the proposed cationic catalytic intermediates were detected by the use of *in situ* mass spectrometry.

2. Experimental

2.1. Materials

All manipulations of air/moisture sensitive compounds were carried out under an atmosphere of argon or nitrogen using standard Schlenk techniques or in an argon atmosphere in a Saffron glove box. All reagents were obtained from major suppliers. Synthesis of complexes **1a,b** has been described previously[19] and crystals could be grown by evaporation of dichloromethane/acetonitrile solutions. $CrCl_3(THF)_3$[3] and complexes **1c,d**[10] were prepared in analogy to methods described previously. 1,2-difluorobenzene was dried with molecular sieves, degassed, vacuum transferred and stored over molecular sieves in the glove box. Other dry solvents were obtained from the Innovative Technology Solvent Purification System (SPS).

2.2. Instrumentation and Characterisation Procedures

NMR spectra were obtained on a Bruker AVII+ 500 NMR spectrometer [500MHz (^{1}H), 125MHz (^{13}C), 470MHz (^{19}F)] at 298K. All ^{13}C spectra are H decoupled unless otherwise stated. Shift values are quoted in ppm relative to TMS or set internal solvent signals. Coupling constants and line widths at half height (W) are quoted in Hz. NMR spectra are often taken without the use of deuterated solvent and referenced to the solvent signal externally referenced to TMS. The shift of 1,2-difluorobenzene (PhF_2) was set to 6.976 (^{1}H), 117.98 (^{13}C) and -139.4 (^{19}F) ppm determined for neat solvent relative an added trace of TMS. Effective magnetic moments were measured using the Evans method and corrected for the diamagnetic contribution.[20,21]

Routine mass spectra were obtained using a micrOTOF electrospray time-of-flight (ESI-TOF) mass spectrometer (Bruker Daltonik) using acetonitrile as a solvent collecting data in positive mode. The peaks quoted correspond to the calculated exact mass, the correct isotope patterns are present where the peak is quoted. For metal complexes a small amount of $Me_3N{\cdot}HCl$ was added to obtain a predictable ion formation ($M+C_3H_{10}N^+$) unless otherwise stated.

Elemental analysis was performed on an Exeter Analytical CE440 Elemental Analyzer by Mr. A. K. Carver in the University of Bath, Department of Chemistry, or externally by London Metropolitan University Elemental Analysis Service, UK.

GCMS analysis was performed with an Agilent 7890B with Agilent 5977A MSD and FID detectors. A DB-FFAP column 30 m in length, with a diameter of 0.250 mm and a 0.25 µm film thickness was used in all cases. A ramp rate of 3°C per minute was used from 40°C to 350°C.

2.3. X-ray Crystallographic Analysis

Intensity data for all structures were collected at 180(2) K on a STOE IPDS (**1b**), and at 150K on a Nonius KappaCCD diffractometer (**3** and **4b**) or a RIGAKU SuperNova (**1a**, **4a**, **$CrCl_3(THF)_3$**) equipped with an Oxford Cryostream. Data were processed using the STOE- [22], Nonius-[23] and RIGAKU Software [24]. For all structures a symmetry-related (multi-scan) absorption correction had been applied. Crystal parameters and details on data collection, solution and refinement for the complexes are provided in Table 2 and for $[Cr(H_2O)_6](OTf)_3{\cdot}3H_2O$ in Table S2. Structure solution, followed by full-matrix least squares refinement was performed using the WINGX-1.80 suite of programs throughout.[25]

2.4. Preparation

*2.4.1. Synthesis of $(Pr_2CHCH_2)_3TACCrCl_3$ (**1c**)*

2.4.1.1. Synthesis of methyl 2-cyano-2-propylpentanoate ($MeOC(=O)C(Pr)_2CN$)

Sodium methoxide (12.00 g, 222 mmol) was dissolved into 100 mL of dry methanol under nitrogen, with the evolution of a considerable amount of heat. Half (50 mL) of the base solution was added drop-wise to ethyl cyanoacetate (11.7 mL,110 mmol, 12.44 g) and the solution left to stir for 15 minutes, leading to a yellowing of the mixture. 1-Bromopropane (10 mL, 110 mmol, 13.54 g) was then added. The system was kept under nitrogen for three hours with vigorous stirring, leading to a cloudy orange solution. The second half of base solution was then added followed by another 10 mL of 1-bromopropane and the mixture left stirring overnight. The vivid red suspension was allowed to cool to room temperature before being decanted from the white precipitate. The salts were extracted with petroleum ether (3 x 100 mL) and the solvent of the combined extractions removed under reduced pressure. The resulting liquid was vacuum transferred at 10^{-2} mbar and 300 ˚C using a water bath to cool the collection vessel. 16.8 g (92 mmol, 84%) of a clear liquid was collected. ^{1}H NMR ($CDCl_3$): δ = 3.79 (3H, s, -OC**H**$_3$), 1.87 (2H, t of d, J = 13.1/4.8, -C**H**$_2$Et), 1.77 (2H, t of d, J = 12.8/4.0, -C**H**$_2$Et), 1.58 (2H, m, -C**H**$_2$Me), 1.33 (2H, m, -C**H**$_2$Me), 0.96 (6H, t, J = 7.3, -C**H**$_3$). ^{13}C NMR ($CDCl_3$): δ = 169.09 (-**C**=O), 118.56 (-**C**N), 52.49 (-O**C**H$_3$), 49.35 (-**C**(Pr)$_2$CN), 38.99 (-**C**H$_2$Et), 18.32 (-**C**H$_2$Me), 13.06 (-**C**H$_3$).

2.4.1.2. Synthesis of 2-propylpentanenitrile (Pr_2CHCN)

De-ionised water (2.5 mL, 2.48 g, 138 mmol) was dissolved into 100 mL of DMSO. Lithium chloride (11.73 g, 277 mmol) was then dissolved into the mixture (very exothermic!) and the system was put under nitrogen. Once dissolved, $MeOC(=O)C(Pr)_2CN$ (16.81 g, 92 mmol) was added and the mixture heated to 150 ˚C whilst stirring overnight. The resulting brown solution was decanted off the yellow solids and 100 mL de-ionised water was added. The aqueous solution was then extracted with pentane (100 mL), which was washed with further de-ionised water (3 x 100 mL). The water washings were extracted with pentane (25 mL) which was then combined with the original pentane solution. The solvent was removed under reduced pressure to give a yellow oil. This was vacuum transferred (~150

˚C, 10^{-2} mbar, liquid nitrogen bath) to give 8.90 g (71 mmol, 77%) of a colourless oil. ^{1}H NMR ($CDCl_3$): δ = 2.54 (1H, m, -C**H**CN), 1.42-1.62 (8H, m, -C**H**$_2$C**H**$_2$Me), 0.96 (6H, t, J = 7.5, -C**H**$_3$). ^{13}C NMR ($CDCl_3$): δ = 121.70 (-**C**N), 34.04 (-**C**H$_2$Et), 30.80 (-**C**HCN), 20.05 (-**C**H$_2$Me), 13.11 (-**C**H$_3$).

2.4.1.3. Synthesis of 2-propylpentan-1-amine ($Pr_2CHCH_2NH_2$)

$AlCl_3$ (10.69 g, 80.1 mmol) was carefully dissolved into 400 mL of ice-cooled dry Et_2O under a nitrogen atmosphere. $LiAlH_4$ (9.07 g, 240.0 mmol) was then slowly added to avoid excessive boiling of the solvent during the highly exothermic reaction. The grey suspension was stirred for an hour at ambient temperature. A solution of Pr_2CHCN (8.90 g, 71.0 mmol) in dry Et_2O (50 mL) was added drop-wise over 30 minutes and left to stir for half an hour. Significant bubbling was observed on addition of each drop due to the highly exothermic nature of the reaction. After complete addition the mixture was cooled in an ice bath and hydrolysed by the careful addition of 50 mL of water, 50 mL of 20% NaOH in water, 100 mL water and another 100 mL of 20% NaOH solution, in that order. The mixture was stirred vigorously for an hour to ensure complete hydrolysis. The suspension became white over this period. The suspension was left to settle before decanting off the clear Et_2O solution, followed by extractions with Et_2O (3 x 150 mL). The solvent was removed from the combined extracts under reduced pressure. The product was vacuum transferred (2 x 10^{-2} mbar, ~150 ˚C, ice bath) to give 7.05 g (54.6 mmol, 77%) of a colourless oil. ^{1}H NMR ($CDCl_3$): δ = 2.60 (2H, d, J = 5.3, -C**H**$_2$NH$_2$), 1.18-1.38 (9H, m, -C**H**C**H**$_2$C**H**$_2$Me), 1.01 (2H, broad s, -N**H**$_2$), 0.90 (6H, t, J = 7.6, -C**H**$_3$). ^{13}C NMR ($CDCl_3$): δ = 44.70 (-**C**H$_2$NH$_2$), 39.99 (-**C**HCH$_2$NH$_2$), 33.43 (-**C**H$_2$Et), 19.40 (-**C**H$_2$Me), 13.89 (-**C**H$_3$).

2.4.1.4. Synthesis of 1,3,5-tris(2-propylpentyl)-1,3,5-triazinane ($(Pr_2CHCH_2)_3TAC$)

Paraformaldehyde (1.65 g, 55.0 mmol) was added to $Pr_2CHCH_2NH_2$ (7.05 g, 54.6 mmol) in 100 mL toluene. The suspension was stirred for 3 days. During this time the particles were consumed and several droplets of water formed, indicating a complete reaction. The water was removed *via* azeotropic distillation of toluene (3 x 50 mL) and the remaining solvent removed under reduced pressure. The mixture was further dried at 10^{-2} mbar and 150 ˚C for 16 hours. The yield after drying was 6.44 g (15.2 mmol, 90%) of a colourless viscous oil. ^{1}H NMR ($CDCl_3$): δ = 3.26 (6H, broad s, -NC**H**$_2$N-), 2.26 (6H, d, J = 7.2, -C**H**$_2$TAC), 1.43 (3H, m, -C**H**CH$_2$TAC), 1.18-1.38 (24H, m, -C**H**$_2$C**H**$_2$Me), 0.88 (18H, t, J = 7.2, -C**H**$_3$). ^{13}C NMR ($CDCl_3$): δ = 75.48 (-N**C**H$_2$N-), 57.38 (-**C**H$_2$TAC), 35.77 (-**C**HCH$_2$TAC), 34.97 (-**C**H$_2$Et), 19.98 (-**C**H$_2$Me), 14.66 (-**C**H$_3$). *Anal.* Calc. for $C_{27}H_{57}N_3$ (%): C, 55.71; H, 9.87; N, 7.22. Found: C, 55.59; H, 9.99; N, 7.33.

2.4.1.5. Synthesis of $(Pr_2CHCH_2)_3TACCrCl_3$ (**1c**)

$CrCl_3(THF)_3$ (3.71 g, 10.0 mmol) was added to $(Pr_2CHCH_2)_3TAC$ (4.28 g, 10.1 mmol) under an argon atmosphere. The reagents were then dissolved into 20 mL dry DCM and the solution stirred for 2 days. The resulting purple solution was separated by column chromatography, eluting with DCM. The solvent of the purple fractions was removed under reduced pressure and the resulting solid dried for 24 hours under high vacuum, yielding 4.97 g (8.5 mmol, 85%) of a purple solid **1c**. ^{13}C NMR (2w% in

o-$C_6H_4F_2$) : δ = 51.3 (W = 130, -**C**H_2Et), 23.9 (W = 136, -**C**H_2Me), 16.8 (W = 127, -**C**H_3), -39.2 (W = 866, -**C**HPr_2). ESI-MS (m/z) $[C_{27}H_{57}Cl_3CrN_3.C_3H_{10}N]^+$: Calculated exact mass: 640.3836; found: 640.3875. *Anal.* Calc. for $C_{27}H_{57}Cl_3CrN_3$ (%): C, 39.04; H, 6.23; N, 4.55. Found: C, 38.79; H, 6.40; N, 4.36.

*2.4.2. Synthesis of (^{i}Bu$_2$CH)$_3$TACCrCl$_3$ (**1d**)*

2.4.2.1. Synthesis of 2,6-dimethylheptan-4-amine (^{i}Bu$_2$CHNH$_2$)

Ammonium acetate (35.02 g, 454 mmol) was dissolved into MeOH (100 mL) under nitrogen before addition of 10 mL (8.08 g, 56.8 mmol) of 2,6-dimethylheptan-4-one. This was stirred for 90 minutes at room temperature. Sodium cyanoborohydride (2.58 g, 41.0 mmol) was dissolved into MeOH (20 mL) and added to the reaction mixture which was left stirring overnight at 30 °C. The reaction vessel was placed in a cold water bath and a liquid nitrogen cooled trap was added. 10 mL of 32% aqueous HCl was added dropwise over the course of 30 minutes, leading to a highly exothermic reaction and considerable white precipitate. CARE: Hydrolysis of the cyanoborohydride leads to the evolution of hydrogen cyanide which should be caught in the trap and disposed of properly. The MeOH was removed under reduced pressure to give a white slurry. This was extracted with pentane (3 x 50 mL) and Et_2O (3 x 50 mL) and the solvents again removed to give a clear oil. This was dissolved in Et_2O (50 mL) before addition of 5.32 g (133 mmol) of NaOH. The mixture was stirred for 2 hours before addition of 5 mL of water to form two phases and dissolve the solids. The organic phase was removed and collected and the aqueous phase extracted with Et_2O (3 x 50 mL) and pentane (2 x 50 mL). The solvent was then removed at reduced pressure. The resulting oil was distilled at 160 °C and 300 mbar to give 5.44 g (38 mmol, 67%) of a colourless non-viscous oil. ^{1}H NMR ($CDCl_3$): δ = 2.83 (1H, quintet, J = 6.6, -C**H**NH_2), 1.73 (2H, nonet, J = 6.7, -C**H**Me_2), 1.17 (4H, m, -C**H**$_2$CMe_2), 0.90 (12H, t, J = 6.4, -C**H**$_3$). ^{13}C NMR ($CDCl_3$): δ = 47.99 (-**C**H_2CMe_2), 46.24 (-**C**HCH_2NH_2), 24.44 (-**C**HMe_2), 23.24 (-**C**H_3), 21.79 (-**C**H_3).

2.4.2.2. Synthesis of 1,3,5-tris(2,6-dimethylheptan-4-yl)-1,3,5-triazinane ((^{i}Bu$_2$CH)$_3$TAC)

Paraformaldehyde (1.03 g, 34.4 mmol) was added to ^{i}Bu$_2$CHNH$_2$ (4.93 g, 34.4 mmol) in 100 mL toluene. The suspension was stirred for 2 days. During this time the particles were consumed and several droplets of water formed, indicating a complete reaction. The water was removed *via* azeotropic distillation of toluene (3 x 50 mL) and the remaining solvent removed under reduced pressure. The mixture was further dried at 50 mbar and 50 ˚C for 6 hours. The yield after drying was 4.00 g (25.7 mmol, 75%) of a colourless viscous oil. NMR spectroscopy indicated a mixture of imine and triazacyclohexane was formed at a ratio of 3:2.

Imine: ^{1}H NMR ($CDCl_3$): δ = 7.35 (1H, d, J = 17.4, =C**H**-*cis*), 7.14 (1H, d, J = 17.4, =C**H**-*trans*), 3.06 (1H, m, -C**H**N=CH_2), 1.24 (2H, m, -C**H**Me_2), 1.05 (4H, d of t, J = 13.7/7.0, -C**H**$_2$CMe_2), 0.86/0.83 (6H/6H, d/d, J = 6.5/6.5 -C**H**$_3$). ^{13}C NMR ($CDCl_3$): δ = 250.91 (-N=**C**H_2), 68.63 (-**C**HN=CH_2), 40.51 (-**C**H_2CMe_2).

Triazacyclohexane: ^{1}H NMR ($CDCl_3$): δ = 3.48 (6H, s, -NC**H**$_2$N-), 2.62 (3H, quintet, J = 6.9, -C**H**N), 1.69 (2H, m, -C**H**Me_2), 1.46 (4H, m, -C**H**$_2$CMe_2), 0.88/0.87 (6H/6H, d/d, J = 6.8/6.8, -C**H**$_3$). ^{13}C

NMR, $CDCl_3$: δ = 67.39 (-N**C**H_2N-), 56.46 (-**C**HN), 45.36 (-**C**H_2CHMe_2). Six further ^{13}C peaks were observed which represent (-**C**HMe_2) and the pairs of (-**C**H_3) for each molecule. These were not assigned but were recorded at 24.98, 24.24, 23.59, 23.13, 22.88 and 21.54. *Anal.* Calc. for $C_{30}H_{63}N_3$ (%): C, 57.73; H, 10.17; N, 6.73. Found: C, 57.66; H, 10.28; N, 6.86.

*2.4.2.3. Synthesis of (^{i}Bu$_2$CH)$_3$TACCrCl$_3$ (**1d**)*

$CrCl_3(THF)_3$ (3.23 g, 8.7 mmol) was added to the (^{i}Bu$_2$CH)$_3$TAC / ^{i}Bu$_2$CHNCH$_2$ mix (4.00 g) under an argon atmosphere. The reagents were then dissolved into 20 mL dry DCM and the solution stirred for 2 days. The resulting purple solution was separated by column chromatography, eluting with DCM. The solvent of the purple fractions was removed under reduced pressure and the resulting solid dried for 24 hours at 50 °C under high vacuum, yielding 3.81 g (6.1 mmol, 71%) of a purple solid. ^{13}C NMR ($CDCl_3$): δ = 37.64 (W = 111, -**C**HMe_2), 28.55 (W = 91, -**C**H_3), 20.16 (W = 32, -**C**H_3), -36.4 (W = 1490, -**C**H_2^{i}Pr). ESI-MS (m/z) of $[C_{30}H_{63}Cl_3CrN_3.C_3H_{10}N]^+$: Calculated exact mass: 684.4276; found: 684.4388. *Anal.* Calc. for $C_{30}H_{63}Cl_3CrN_3$ (%): C, 41.07; H, 6.58; N, 4.35. Found: C, 40.86; H, 6.72; N, 4.33.

2.4.3. Synthesis of $Cr(OTf)_3$ **2**

Trifluoromethanesulphonic acid (32.64 g, 19.2 mL, 218 mmol) was dissolved into de-ionised water (75 mL) by drop-wise addition due to the highly exothermic reaction. Considerable fuming was observed on addition of each drop. Granulated chromium (4.16 g, 80 mmol) was then added and stirred vigorously with no initial reaction observed. The solution was heated to 90 °C in the presence of oxygen and over the course of 48 hours became blue/violet in colour, indicative of $[Cr(H_2O)_6]^{3+}$ formation. The solution was filtered through sintered glass to remove the excess chromium before the solvent was removed under reduced pressure to give a viscous blue oil. Further drying of some of the viscous oil in a desiccator with P_4O_{10} for a week resulted in highly hygroscopic blue crystals of $[Cr(H_2O)_6](OTf)_3{\cdot}3H_2O$ suitable for X-ray crystallography. The oil was heated to 100 °C under reduced pressure for one hour, leading to a pale green solid. Further heating to 200-300 °C in a regeneration oven under high vacuum (10^{-2} mbar), led to a dark green solid and a considerable quantity of water being collected over the course of an hour. The product demonstrated strong hydrophilicity, reverting back to a blue/green oil within seconds of exposure to air. The solid was ground by pestle and mortar under an argon atmosphere to give an extremely fine powder, which was further dried, under high vacuum. After drying, 32.2 g (64.4 mmol, 89%) of a green powder **2** was collected. *Anal.* Calc. for $C_3CrF_9O_9S_3$ (%): C, 7.22; H, 0.00. Found: C, 7.12; H, 1.17. This experimental value would suggest 0.4 H_2O (C%) or 2.9 H_2O (H%) per chromium and may be due some residual water and/or uncertainty in the analytical method including sample preparation of the highly hygroscopic product.

Alternative synthesis from CrO_3: 10g water is cooled in an ice bath and 17.3g triflic acid (M=150, 0.115mmol) added slowly (warm!). Then 3.76g CrO_3 (M=100, 0.0376mmol) are added, residues washed in with a few more ml water, followed by ca 20ml ^{i}PrOH (slow, gets hot!). After one hour, the deep blue solution is concentrated on the rotary evaporator (50mbar, 50 ºC) for 2 hours and then at high vacuum with bridge and LN2 cooled Schlenk flask. When the solution solidifies the temperature is slowly raised as above while the solids turn light green. It was found that (probably due to organic residues) this solid tends to give dark products on heating above 200 ºC.

2.4.4. Synthesis of $Cr(OTf)_3(THF)_3$ **3**

A Schlenk flask with 555mg of $Cr(OTf)_3$ (**2**) (M=499, 1.11mmol) is evacuated and THF (from NaK, ca 10ml) is condensed in. The dark solution is stirred for 4hrs (occasional warming in hot water bath as it becomes more viscous) and then all volatiles are pumped off (high vacuum, 40 ºC). The sticky solids are dissolved in ca 10 ml of o-difluorobenzene (slow to dissolve and very viscous at first). After 2hrs of stirring, the now more fluid green solution is filtered and then left in a -20 C freezer for two days. Some **3** crystallised out. The solution is decanted and the residue washed with two 5ml portions of hexane. The combined solution, washings and further 20ml of hexane are left in the freezer to obtain additional 160mg product. The combined solids are dried in vacuo to give 360mg of a light green solid **3** (for M=715.5: 0.50mmol, 45%). Anal. calcd for $C_{15}H_{24}CrF_9O_{12}S_3$ (%): C, 25.18; H 3.38. Found: C, 25.09; H, 2.85.

NMR: 34.6mg are dissolved in 1438mg PhF_2:

^{1}H: -0.51 (β-CH_2 of THF, W=655Hz), α-CH_2 too broad to be observed; $\mu_{eff}=3.74\mu_B$ (Evans method)

^{13}C: -84.5 (β-CH_2 of THF, W=3300Hz), α-CH_2 too broad to be observed

^{19}F: -74.4 (3F, W=510Hz), -77.7 (6F, W=550Hz)

2.4.5. Synthesis of $Cy_3TACCr(OTf)_3$ **4a**

Route A: $Cy_3TACCrCl_3$ (**1a**) (1.982 g, 4.03 mmol) is weighed out into a Schlenk tube, and then removed from the glove box and connected to a Schlenk flask containing triflic acid (TfOH). The Schlenk tube is then placed in liquid nitrogen and the TfOH condensed over. After condensing over all the acid, it is condensed back over to yield a sticky dark blue solid which is then washed with diethyl ether 10 times, by vacuum transferring it over then decanting the washings back across, until the ether appeared colourless. The dark blue solid is then dried on a vacuum line to yield 3.083 g of **4a** (Yield = 92%). *Anal.* Calc. for $C_{24}H_{39}CrF_9N_3O_9S_3$ (%): C, 34.62; H, 4.72; N, 5.05. Found: C, 34.53; H, 4.89; N, 4.92. UV/Vis(KBr, cm^{-1}): 15120, 21500.

Route C: 34.6mg of $Cr(OTf)_3(THF)_3$ (0.0484mmol) are dissolved in 1438mg of o-difluorobenzene in an NMR tube and Cy_3TAC (M=333.56, 16mg, 0.048mmol) is added – no visible change at first! After 1 hr turquoise crystals cover the walls of the NMR tube. Shaken down the much lighter solution is taken to NMR: nearly 2.5eq THF are shown with little (<0.002mmol, 0.04eq) Cy_3TAC left.

2.4.6. Synthesis of $Bz_3TACCr(OTf)_3$ **4b**

Route B: 20mg Bz_3TAC (0.056mmol) and 28mg $Cr(OTf)_3$ (0.056mmol) are stirred with 945mg of o-difluorobenzene. After 4hrs, the largely dissolved mixture is filtered and the filtrate placed into vial with hexane. The filter is extracted with further two 1ml portions of o-difluorobenzene and placed in another vial with hexane and a final o-difluorobenzene extract is placed into a freezer to give crystals good enough for X-ray crystallography. Further product is obtained from the hexane vials.

Route A: 238mg of $Bz_3TACCrCl_3$ (**1b**) (0.46mmol) are dissolved in 3.5g TfOH which is subsequently distilled off. The residue is washed with Et_2O (5ml) to give 356mg (91%) of **4b**, m.p. 207-208C. *Anal.*

Calc. for $C_{27}H_{27}CrF_9N_3O_9S_3$ (%): C, 37.85; H, 3.18; N, 4.90; S, 11.23; Cr, 6.07. Found: C, 36.48; H, 3.13; N, 4.63; S, 11.04; Cr, 6.65. UV/Vis(KBr, cm^{-1}): 16660, 23370.

2.4.7. Synthesis of $(Pr_2CHCH_2)_3TACCr(OTf)_3$ (**4c**)

$(Pr_2CHCH_2)_3TACCrCl_3$ (**1c**) (1.97 g, 3.4 mmol) was evacuated and cooled with liquid nitrogen and approximately 10 mL of triflic acid was condensed onto the purple solids across all-glass linkages. The acid was then allowed to melt and the system opened up to a trap cooled with liquid nitrogen to catch any hydrogen chloride given off. Once the acid melts a fast reaction proceeds with considerable effervescence. Once the reaction was complete the acid was distilled off at 40 °C and 10^{-2} mbar over the course of a day. The dark blue solids were then washed twice with 25 mL of dry Et_2O under a nitrogen atmosphere to remove any further acid. Subsequent drying at reduced pressure led to 2.73 g (3.0 mmol, 88%) of a pale blue solid **4c**. ^{13}C NMR (1w% in *o*-$C_6H_4F_2$): δ = 42.32 (W = 83, -**C**H_2Et), 19.21 (W = 41, -**C**H_2Me), 13.57 (W = 37, -**C**H_3), -43.9 (W = 5100, -**C**HPr_2). ^{19}F NMR (*o*-$C_6H_4F_2$): δ = -45.56 (W = 3300). *Anal.* Calc. for $C_{30}H_{57}CrF_9N_3O_9S_3$ (%): C, 39.04; H, 6.23; N, 4.55. Found: C, 38.81; H, 6.38; N, 4.32.

2.4.8. Synthesis of $(^iBu_2CH)_3TACCr(OTf)_3$ (**4d**)

$(^iBu_2CH)_3TACCrCl_3$ (**1d**) (1.06 g, 1.7 mmol) was cooled with liquid nitrogen and approximately 10 mL of triflic acid was condensed onto the purple solids across all- glass linkages. The acid was then allowed to melt and the system opened up to a trap cooled with liquid nitrogen to catch any hydrogen chloride given off. Once the acid melts a violent reaction proceeds with considerable effervescence. Once the reaction was complete the acid was distilled off at 40 °C and 10^{-2} mbar over the course of a day. The dark blue solids were then washed four times with 25 mL of dry Et_2O under a nitrogen atmosphere to remove any further acid. Subsequent drying at reduced pressure led to 1.43 g (1.5 mmol, 87%) of a pale blue solid **4d**. ^{13}C NMR (*o*-$C_6H_4F_2$): δ = 37.3 (W = 320, -**C**HMe_2), 20.3 (W = 120, -**C**H_3), 19.6 (W = 150, -**C**H_3), -30.1 (W = 2740, -**C**$H_2{}^iPr$). ^{19}F NMR (*o*-$C_6H_4F_2$): δ = -50.3 (W = 2400). *Anal.* Calc. for $C_{33}H_{63}CrF_9N_3O_9S_3$ (%): C, 41.07; H, 6.58; N, 4.35. Found: C, 40.90; H, 6.75; N, 4.34.

2.5. Typical catalysis of 1-hexene trimerisation

2.5.1. NMR observation:

Trimerisation was observed by ^1H NMR and quantified by integration (relaxation delay of at least 20s was used to ensure full relaxation) of four regions: A is the integral of the =CH- signal of 1-hexene at about 5.8 ppm, B is the integral of the remaining olefinic signals at 4.5-5.5 ppm, C is the integral of the whole hexene region from 6.0-0.5 ppm and D is the Al-CH_2 region at around 0.0-0.5 ppm (not including Al-Me). Integral C is set to 1200+x with x as 1.5×D for $AlEt_3$ or 3.5×D for Al^iBu_3 (taking into account the remaining signals of AlR_3 in the hexene region). As all olefins have 2H per molecule in the region B, it can be shown that the % 1-hexene remaining is A, the % trimer formed is 0.75×(200-B) and the % isomers formed is 100-A-0.75×(200-B).

$Cy_3TACCr(OTf)_3$ (**4a**) (5.1mg, 0.0061mmol) is suspended in 315.7mg of 1-hexene (3.76mmol, 614eq) and 394 mg of o-difluorobenzene (3.45mmol, 564eq). Then Me_3Al (9 mg weighed into a pipette (0.125mmol, 20eq) is added. All dissolves first to a blue/turquoise and then within minutes to a light green solution and is transferred into an NMR tube. ^{19}F NMR after 25min shows 2.7eq OTf at -76ppm.

NMR after 3hrs shows 91% hexene left, 9% trimer (55 turnover per Cr) and no isomer (0.17eq CH_4 at 0.15ppm, 0.062mmol $AlMe_3$ or about half of added $AlMe_3$ at -0.22ppm, additional Al-Me at 0.2 (0.018mmol Me or 3.0eq per Cr) and 0.0ppm (0.011mmol or 1.9eq per Cr)), . Thus, very slow progress. The colour had changed to more blueish green after 3 hrs.

After 24hrs: 30.4% hexene, 67.6% trimer and 2.0% isomer (5% conversion in last hour!)

After 48hrs: 3.8% hexene left with 89.2% trimer and 7% isomer.

2.5.2. Comparison of activation with $AlMe_3$, $AlEt_3$ and Al^iBu_3:

$(Pr_2CHCH_2)_3TACCr(OTf)_3$ (**4c**) (16.3mg, 0.0177mmol) is dissolved in 3.10g of o-difluorobenzene. 1.04g each (0.0059mmol Cr) of this solution is added to the following:

A: $AlMe_3$ (46mg, 0.64mmol, 108eq) and 1-hexene (620mg, 7.4mmol, 1250eq); NMR next day: 91.9% 1-hexene, 6.1% trimer, 2.0% isomers;after 5d: 84.5%, 7.4%, 7.2% - 0.0016mmol or 27% of **3d** at 4.23d (3H, ring), 3.66d (3H, ring), 2.69d (6H, α-CH_2) – ^{13}C by HSQC and HMBC:74 (ring), 57 (α-CH_2) and 35ppm (β-CH) as visible signals of the triazacyclohexane transferred to aluminium.

Additional observable signals in ^1H: 0.15ppm (CH_4, about 2eq per Cr; HSQC ^{13}C: -4.5ppm); apart from a larger signal at -0.30ppm for Al-Me, an additional set of signals at 0.18dd (5.1 and 14.0 Hz) and -0.01dd (8.0 and 14.0 Hz) is detected for α-CH_2 (HSQC ^{13}C: 21.7ppm (C_1)) of about 6eq per Cr of Al-CH_2CHMeBu; further ^{13}C signals from long range HMBC: 23.7 (Me-C_7), 30.3 (C_2) and 41.8 (C_3) ppm [26]

B: $AlEt_3$ (83mg, 0.73mmol, 124eq) and 620mg 1-hexene (620mg, 7.4mmol, 1250eq); NMR next day: 54.1% 1-hexene, 38.1% trimer, 7.8% isomers; after 4d: 4.9%, 59.3%, 35.9% - 0.0015mmol or 25% of **3d** at 4.28d (3H, ring), 3.57d (3H, ring), 2.69d (6H, α-CH_2) – ^{13}C by HSQC and HMBC:75 (ring), 58 (α-CH_2) and 35ppm (β-CH) as visible signals of the triazacyclohexane transferred to aluminium.

Additional observable signals: ethane can be detected as ^1H-^{13}C-HSQC cross peak at 0.81ppm (^1H) and 7.18ppm (^{13}C), apart from a large set of signals for $AlEt_3$ at 1.10t and 0.31q (^{13}C-HSQC at 9.1 and 1.3ppm, respectively),

C: Al^iBu_3 (120mg, 0.61mmol, 103eq) and 1-hexene (578mg, 6.9mmol, 1160eq); NMR after 4 hrs: 5.5% 1-hexene, 29.5% trimer, 65.0% isomers; after 4d: 0.7%, 29.3%, 70.0% - 0.0037mmol or 63% of **3d** at 4.31d (3H, ring), 3.55d (3H, ring), 2.71d (6H, α-CH_2) – ^{13}C by HSQC and HMBC:75 (ring), 58 (α-CH_2) and 35ppm (β-CH) as visible signals of the triazacyclohexane transferred to aluminium.

Additional observable signals in ^1H: 0.31d for α-CH_2 of ^{i}Bu-Al (HSQC ^{13}C: 25.7ppm (C_1) – HMBC: 28.0 (C_2 and C_3)) and an additional signal at 0.45t (HSQC ^{13}C: 13.4 (CH_2) with further ^{13}C signals from long range HMBC: 26.1 (C_2) and 36.5 (C_3) ppm matching those observed for $^iBu_2$Al-hexyl [27].

Tests for mixed AlR_3:

Et_2AlMe: 20mg of $AlMe_3$ (0.277mmol), 63mg of $AlEt_3$ (0.552mmol), 1786mg of o-difluorobenzene (15.65mmol) and 1560mg of 1-hexene (18.5mmol) are mixed and checked by ^1H NMR: based on 15.65mmol o-difluorobenzene it contained 18.0mmol of hexene (17.6mmol 1-hexene), 0.49mmol of $AlEt_3$ at 1.03t and 0.14q ppm, 0.26mmol of $AlMe_3$ at -0.004 (0.70mmol bridge Me), -0.13 (0.07mmol) and -0.8 (0.01mmol). 590mg of the mixture (0.048mmol of $AlMe_3$, 0.095mmol of $AlEt_3$, 2.692mmol of o-difluorobenzene, 3.188mmol of hexene) is added to 7.5mg of **4c** (0.0081mmol). NMR after 10hrs:

37% hex, 58% trim, 5% isom, 0.0010mmol/17% TACAl; after 3d: 11% hex, 71% trim, 18% isom, 0.0015mmol/25% TACAl; after 9d: 0.3% hex, 74.6% trim, 25.1% isom, 0.0028mmol/47% TACAl at 4.23, 3.63 and 2.69ppm. After 18d, the contents of the NMR tube is distilled in air to isolate the volatile solvent and hexenes: contains 15w% hexenes, 0.7w% hexane and hexene isomer: 67% trans-2-hexene, 17% cis-2-hexene, 14% trans-3-hexene, 2% cis-3-hexene.

$^{i}Bu_2AlMe$: Preparation of a 1-hexene/o-difluorobenzene solution of $^{i}Bu_2AlMe$: 57mg of $Al^{i}Bu_3$ (0.287mmol), 10.5mg of $AlMe_3$ (0.1457mmol), 3496mg of 1-hexene (41.54mmol) and 2096mg of o-difluorobenzene (18.37mmol) are mixed and checked by NMR: contains relative to 18.37mmol of o-difluorobenzene: 40.8mmolof hexene (39.8mmol 1-hexene, rest isomers), 0.254mmol of $^{i}Bu_3Al$ and 0.139mmol $AlMe_3$; ^{1}H NMR of $Al^{i}Bu$ at 0.143d, AlMe at 0.022br in 4:3 ratio.

About 4mg of **4c** are dissolved in 650mg of this solvent mix (0.033mmol/9 eq $Al^{i}Bu_3$; 0.017mmol/5 eq $AlMe_3$; 4.77mmol/1300 eq hexene) and observed by NMR. Proceeds well – after 4d: 13.4% hexene, 69.2% trimer and 17.5% isomer – ^{19}F NMR after 5d shows 0.0407mmol OTf at -77.7ppm relative to 2.11mmol of o-difluorobenzene, thus, 0.0036mmol Cr – thus, [Cr] = 3.7mM. After 23d: 11% hexene, 73% trimer and 16% isomer, isobutene (4.63 and 1.64ppm) quickly rises to about 0.002 mmol and then more slowly to 0.008mmol at the end (0.5 to 2eq per Cr) – thus nearly 10% of AlR is hexyl. Very little TACAl, about 0.0002mmol or 6% of Cr.

2.5.3. Bulk synthesis:

1-hexene (30 g, 0.357 mol) was weighed out in a 500 mL round bottomed flask, triethyl aluminium ($AlEt_3$) (0.163 g, 1.43 mmol) was then added to the flask and the solution was allowed to stir for 1 hour. In a separate flask $Cy_3TACCr(OTf)_3$ (**4a**) (0.1981 g, 0.238 mmol) was weighed out along with $AlMe_3$ (2.45 wt. % in toluene, 2.099 g, 0.714 mmol) and o-difluorobenzene was added as a solvent for the catalyst dissolution (11.568 g, 0.101 mol) and the solution left to stir for 1 hour. After leaving both solutions to stir, they were combined in a 500 mL round bottomed flask and left to stir overnight. By NMR, the conversion to trimer was found to be 26.2 % from the original 1-hexene added, with no isomerisation seen. The remaining 1-hexene was removed by vacuum transfer and reused in a second reaction, with the 1-hexene recovered (16.381 g, 0.195 mol), triethyl aluminium (0.111 g, 0.974 mmol) was added to this 1-hexene. In a separate flask: $Cy_3TACCr(OTf)_3$ (0.081 g, 97.4 μmol), $AlMe_3$ (2.45 wt. % in toluene, 0.859 g, 0.29 mmol) and o-difluorobenzene (16.2 g, 0.142 mol) were added together and both solutions left to stir for 1 hour, before then combining the two and leaving to stir together overnight. The conversion of 1-hexene to trimer was 28.3 %. Both trimer mixtures were then added together and extracted by phase separation with dilute HCl and pentane. The organic phase was washed several times with dilute HCl and the aqueous phase washed with pentane several times. The organic phases were then combined and dried with $MgSO_4$. The solvent was removed by rotary evaporation, and the remaining liquid high vacuum transferred (100-150 ºC at 10^{-3} mbar) to yield 12.495 g of trimer product (42% isolated yield).

2.6. Air Sensitive Mass Spectrometry Procedure

Direct infusion mass spectrometry analyses were performed using an electrospray time-of-flight (MicroTOFQ) mass spectrometer (Bruker Daltonik GmbH, Bremen, Germany), analyses were performed in ESI positive and negative mode. For positive mode the capillary voltage was set to 4500 V, nebulizing gas at 0.5 bar, drying gas at 3.0 L/min at 110°C. For negative mode the capillary

voltage was set to 4500 V, nebulizing gas at 0.5 bar, drying gas at 4.0 L/min at 200°C.The TOF scan range was from 50 - 2300 mass-to-charge ratio (m/z).

This was coupled to an MBraun glove box containing an argon atmosphere. An air-tight connector in the side of the glove box allowed for PEEK tubing to pass from the glove box to the mass spectrometer without exposure to air or moisture. The sample was injected directly into the tubing *via* syringe and the use of an adaptor. The instrument was calibrated post-acquisition using a range of sodium formate clusters. The observed mass and isotope pattern were considered to match the corresponding theoretical values calculated from the empirical formula when an error of less than 20 ppm was observed. The background spectrum was established before each run with the use of samples of each reagent.

The trimerisation catalysis analysed using the positive ion detection mode was carried out with the use of **4d** (2.5 mg, 2.6 µmol), $AlMe_3$ (2.5 w% in toluene, 4.9 mg, 68 µmol, 26 equivalents), 1-hexene (1.226 g, 14.6 mmol, 5600 equivalents) and *o*-$C_6H_4F_2$ (2.07 g, 18.2 mmol, 7000 equivalents). The reaction analysed using the negative ion detection mode was carried out using very similar conditions, though fewer equivalents of activator were used. A second MS experiment used analogous conditions with only 450 equivalents of 1-hexene.

Analysis of the sample was carried out in two stages, firstly within one minute of activator addition and secondly within one minute of 1-hexene addition. At least three aliquots of *o*-$C_6H_4F_2$ were run through the system before each sample was analysed to reduce the risk of contamination.

3. Results and Discussion

3.1. Synthesis and Characterisation

The substitution of chloride ligands bound to chromium(III) has been described previously with the use of neat trifluoromethanesulphonic acid (TfOH) and in the presence of similar amine based ancillary ligands, ammonia [28] and 1,4,7-trimethyl-1,4,7-triazacyclononane (Me_3TACN) [29]. The methods described were modified and applied to the synthesis of four $R_3TACCr(OTf)_3$ **4** pre-catalysts from their chromium trichloride analogues **1**, Scheme 1. Despite the weaker binding of R_3TAC ligands compared to those previously investigated, the reaction proceeded as expected and near quantitative yields were recorded for a range of differently substituted triazacyclohexanes (route A).

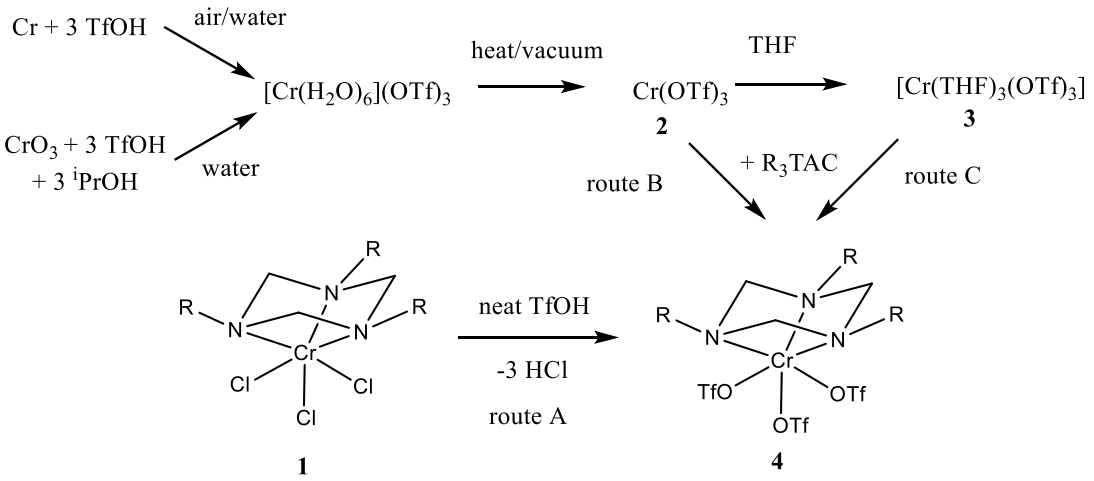

R = cyclohexyl (**a**), benzyl (**b**), $^{n}Pr_2CHCH2$ (**c**), $^{i}Bu_2CH$ (**d**)

Scheme 1. Synthesis of triazacyclohexane triflate complexes **4** and their $Cr(OTf)_3$ precursors.

As anhydrous triflate complexes can often be obtained from aqueous triflates by simple heating under vacuum (e.g. [30]) we also explored a more direct route to the same complexes. Aqueous blue solutions of $[Cr(H_2O)_6](OTf)_3$ were obtained in modification to literature procedures either from aerobic dissolution of chromium metal in aqueous triflic acid or reduction of an aqueous solution of CrO_3 and triflic acid with isopropanol.[31-33] Concentration of the blue solution at high vacuum resulted in a blue viscous oil. Further drying in a desiccator filled with P_4O_{10} resulted in very hygroscopic blue crystals identified as $[Cr(H_2O)_6](OTf)_3 \cdot 3H_2O$ by X-ray crystallography (see supplementary material). Further drying under vacuum with slow heating to 100 °C resulted in a light green $Cr(OTf)_3(H_2O)_x$. Further drying at temperatures slowly increasing to 200 °C resulted in a sudden release of gases at around 160 °C. TGA/MS studies (ESI) on green solids obtained at 130 °C showed a release of water between 160 and 240 °C. Release of a small amount of SO_2 and TfOH is also seen at this temperature range and much more pronounced at 300 to 400 °C indicating decomposition of the triflate anion. Thus, the removal of all water must be done with care to avoid anion decomposition. We found that slow heating to 200 °C followed by suspension of the green product in neat triflic acid with subsequent high vacuum removal at 200 °C resulted in sufficiently pure anhydrous $Cr(OTf)_3$. The product was insoluble in non-coordinating solvents. A good sample could be reacted with Bz_3TAC in o-difluorobenzene to give a turquoise-blue solution of **4b** which gave crystalline product on cooling in a freezer or vapour diffusion of hexane into the filtered solution (route B). In order to avoid problems with contaminants in impure **2**, a well-defined THF complex **3** was obtained by dissolving **2** in dry THF and crystallisation by hexane vapour diffusion (products still containing water or TfOH result in THF polymerisation). X-ray crystallography showed that **3** is the triflate analogue of meridional $CrCl_3(THF)_3$. Figure 1 shows the molecular structure of **3** and some selected bond distances and angles along with the corresponding parameters for $CrCl_3(THF)_3$. While the crystal structure of the chloride analogue $CrCl_3(THF)_3$ has previously been published at 100 K [34] and 278 K [35], we obtained a structure at the same temperature as used for **3** (150 K) at a better R value (4.2% vs 7.4% and 5.9%, respectively) used for this comparison to **3**. The Cr-O(THF) bond distances are significantly shorter in **3** compared to the chloride complex and the THF ligands are more compressed in $CrCl_3(THF)_3$ than in **3** based on the THF-Cr-THF angles. Thus, as expected OTf is much weaker trans-labilising and exerts a small steric effect on the other ligands than chloride. Quantitative NMR spectra in PhF_2 show a single paramagnetically broadened and shifted NMR signal for the β-CH_2 groups in THF in both ^{1}H and ^{13}C as well as two resolved 500 Hz

wide ^{19}F NMR signals (1:2 ratio) for the two inequivalent triflate groups in nearly the correct amount relative the solvent signals.

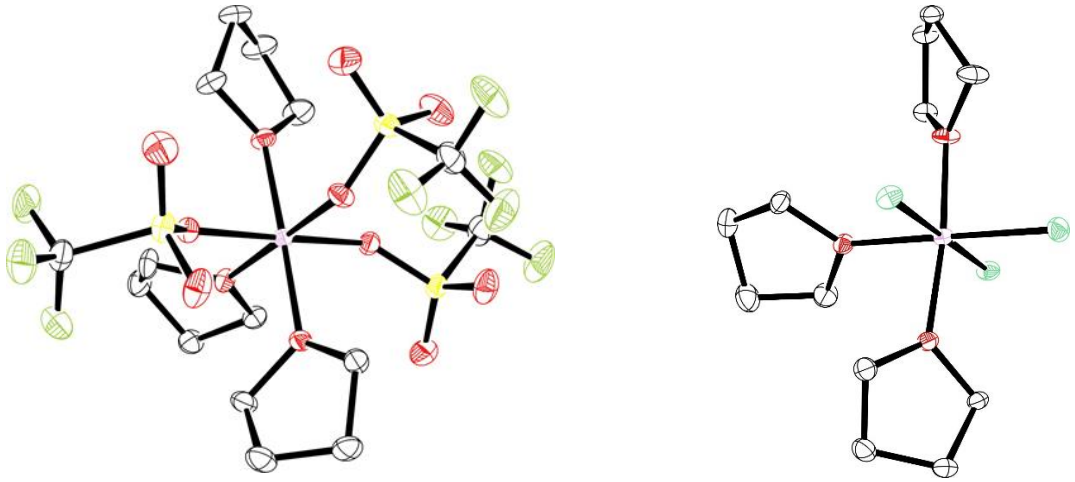

Figure 1. ORTEP representation of the molecular structures of **3** and **$CrCl_3(THF)_3$** with hydrogen atoms omitted for clarity and atoms are drawn at 30% probability. Selected bond distances for **3**: Cr-OTf (trans THF) 1.953(3), Cr-OTf (trans OTf) 1.959(2) and 1.951(2), Cr-O_{THF} (trans OTf) 2.000(2), Cr-O_{THF} (trans THF) 1.982(2) and 1.990(2). Selected bond angles: O_{THF}-Cr-O_{THF}: 178.45(11), 89.67(10), 89.03(10); OTf-Cr-OTf: 175.54(11), 92.49(11), 91.18(11). For comparison, **$CrCl_3(THF)_3$**: Cr-O(trans THF) 2.0041(14) and 2.0279(14), Cr-O (trans Cl) 2.0747(15), Cr-Cl (trans Cl) 2.3130(6) and 2.3205(6), Cr-Cl (trans THF) 2.2931(6). Selected bond angles: O-Cr-O: 173.42(6), 87.98(6), 85.56(6); Cl-Cr-Cl 177.03(2), 90.81(2), 91.74(2) (disorder in one THF not shown)

Complex **3** is a suitable precursor for the near quantitative synthesis of complexes **4** by addition of one equivalent of triazacyclohexane in o-difluorobenzene (route C). In the case of poorly soluble **4a**, crystals suitable for X-ray diffraction grew within one hour of addition leaving a solution containing nearly three equivalents of THF and negligible amounts of remaining ligand as determined by NMR.

The more soluble compounds **4c,d** were characterised using paramagnetic ^{13}C and ^{19}F NMR spectroscopy. The broadened ^{13}C NMR spectrum was little changed on substitution of the chloride ligands and follows the trends previously observed for differently substituted complexes **3** [3]. A broad peak could be observed for **4** by ^{19}F NMR spectroscopy indicative of inner sphere co-ordination of three triflate ions. In this manner both the chloride substitution and the R_3TAC retention could be confirmed.

3.1.1. Crystal structures of **4a**,**b** and **1a,b** for comparison

Complexes **4a** and **4b** have been characterised by X ray crystallography. Crystals of the known [19] analogous chloride complex **1a** and **1b** have been obtained by crystallisation from acetonitrile/dichloromethane or methylene chloride, respectively, and comparison allows a direct assessment of the effect of the different anionic ligand. Complexes **4a** and **4b** crystallise with half and a full molecule of PhF_2, respectively, and disorders in the triflate groups in **4a** while **1a** crystallises without solvent and **1b** with 2.5 molecules of CH_2Cl_2 per complex in the crystal lattice and a disorder in one of the benzyl groups. The molecular structures with the solvent molecules and disorders removed are shown in Fig 2 and selected average bond distances and angles in Table 1. The Cr-N bond distance are significantly smaller in the triflate complexes compared to the chlorides indicating a significantly

weaker bond to the triflate as found for the THF complexes above and as expected for more weakly coordinating triflate anion.

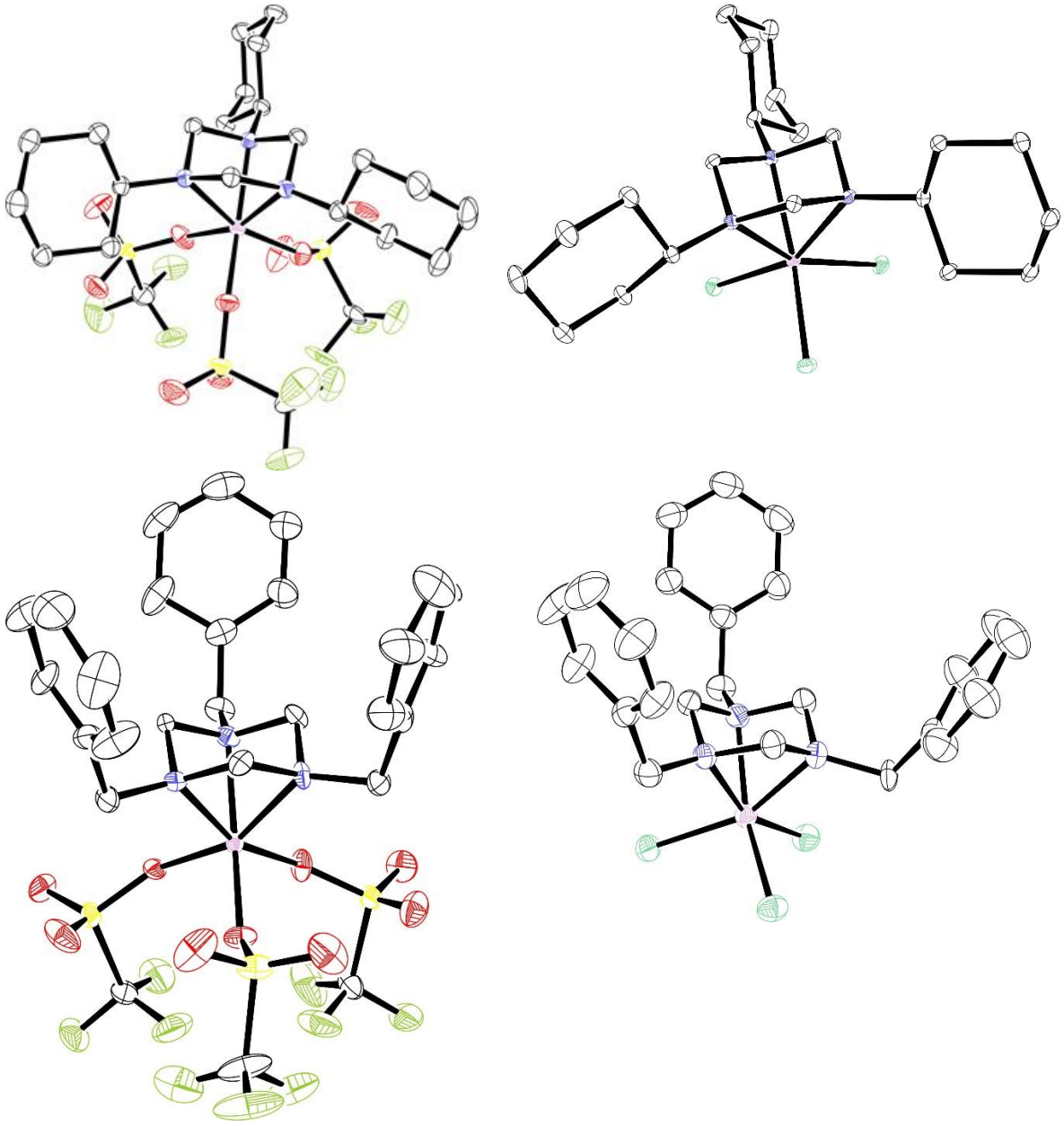

Figure 2. ORTEP representation of the molecular structures of Molecular structures of **4a** (top left), **1a** (top right), **4b** (bottom left) and **1b** (bottom right) with hydrogen atoms and solvent molecules omitted for clarity and atoms are drawn at 30% probability.

Table 1. Selected average bond distances (Å) and angles (°) in **4a**, **1a**, **4b** and **1b**.

complex	**4a**$*(PhF_2)_{0.5}$	**1a**	**4b**$*(PhF_2)$	**1b**$*(CH_2Cl_2)_{2.5}$
Cr-N	2.0777(19)	2.1215(17)	2.078(8)	2.110(4)
Cr-O or Cr-Cl	1.9498(18)	2.2921(5)	1.956(7)	2.2776(14)
N-Cr-N	67.56(7)	65.95(6)	67.2(3)	65.72(15)
Cr-N-C(R)	132.33(14)	132.26(13)	130.8(7)	128.0(2)

O-Cr-O or Cl-Cr-Cl	95.59(9)	99.18(2)	94.2(3)	99.06(6)

Table 2. Summary of X-ray Crystallography for **3, $CrCl_3(THF)_3$, 1a, 1b, 4a, 4b** with selected average bond distances and angles (*indicates range of values or SD, if greater, as a measure of confidence).

Empirical Formula	$C_{15}H_{24}O_{12}F_9CrS_3$ **3**	$C_{12}H_{24}Cl_3CrO_3$ **$CrCl_3(THF)_3$**	$C_{21}H_{39}Cl_3CrN_3$ **1a**	$C_{26.5}H_{32}Cl_8CrN_3$ **1b*$(CH_2Cl_2)_{2.5}$**	$C_{27}H_{41}O_9F_{10}N_3CrS_3$ **4a*$(PhF_2)_{0.5}$**	$C_{33}H_{31}O_9F_{11}N_3CrS_3$ **4b*(PhF_2)**
Formula Weight	715.52	374.66	491.90	2912.60	889.81	970.79
Crystal System	Monoclinic	Monoclinic	Triclinic	Monoclinic	Monoclinic	Orthorhombic
Space Group	P 2_1	P $2_1/c$	P -1	C 2/c	I 2/a	P $2_12_12_1$
Unit Cell Dimensions						
a (Å)	9.0638(2)	8.0382(3)	6.9098(2)	20.727(3)	23.5157(3)	15.3849(6)
b (Å)	14.4268(3)	12.5123(5)	10.6220(3)	11.957(2)	17.3075(2)	15.3679(6)
c (Å)	10.3798(3)	16.3957(5)	16.4715(4)	27.509(4)	18.4883(2)	17.2012(6)
α (°)	90	90	86.641(2)	90	90	90
β (°)	91.2011(10)	92.652(3)	87.888(2)	92.022(14)	100.6390(10)	90
γ (°)	90	90	83.072(2)	90	90	90
V (Å^3)	1356.98(6)	1647.25(10)	1197.51(6)	6813.4(18)	7395.35(15)	4066.9(3)
Z	2	4	2	8	8	4
μ (mm^{-1})	(Mo Kα) 0.769	(Mo Kα) 1.181	(Cu Kα) 7.090	(Mo Kα) 0.985	(Cu Kα) 5.073	(Mo Kα) 0.540
Total Reflections	17202	15267	19245	28777	41721	54270
Independent Reflections (R_{int})	5744 (0.0369)	4437 (0.0495)	4741 (0.0492)	6752 (0.0933)	7317 (0.0330)	9241 (0.1286)
R_1, wR_2 [I > 2σ(I)]	0.0331, 0.0831	0.0417, 0.0967	0.0311, 0.0725	0.0771, 0.1917	0.0452, 0.1130	0.1078, 0.2798
Goodness-of-fit (GOF) on F^2	1.043	1.061	1.058	1.052	1.044	1.250
Largest Difference in Peak and Hole (e/Å^3)	0.374, -0.506	0.530, -0.666	0.297, -0.339	0.835, -0.546	0.764, -0.521	3.373, -1.172

$R_1=\Sigma\ ||Fo|-|Fc||/\Sigma|Fo|$. $wR_2=\{\Sigma[w(Fo^2-Fc^2)^2]/\Sigma[w(Fo^2)^2]\}^{1/2}$. $GOF=S=\{\Sigma[w(Fo^2-Fc^2)^2]/(n-p)\}^{1/2}$.

3.2. Catalysis of α-Olefin Trimerisation

This newly developed procedure enabled the facile two-step synthesis of pre-catalysts **4a-d**, which were then investigated in relation to their activation and catalysis. It was hoped that the weakly co-ordinating nature of the triflate ligands would facilitate alkylation and abstraction during activation. Meanwhile, the disperse charge of these anions was expected to support the formation of a weakly coordinating anion assumed to be essential for high trimerisation activity. To test this hypothesis a range of activating agents were screened in order to determine whether the triflate anions enabled activation by agents less potent than MAO. The activation success was measured by the ability of the resulting species to trimerise 1-hexene, reactivity that has been established previously for $R_3TACCrCl_3$ complexes.

It was found that addition of 5-20 equivalents of AlR_3 (R=Me, Et, iBu) to an o-difluorobenzene suspension of the triflate complexes leads to dissolution to a blue/green solution which trimerises 1-hexene on addition. In the case of $AlMe_3$, there seems to be a significant initiation period of several hours before full activity is reached. This can be rationalised by the requirement for a β-H on the Cr-alkyl for agostic assisted β-H abstraction with reduction to a Cr(I) complex to initiate the trimerisation catalysis. This process may occur in two steps or directly in one step as shown in Scheme 2 and will subsequently referred to as "β-H abstraction". While Et and ^{i}Bu already have a β-H, Me requires an apparently slow insertion of 1-hexene to give a β-H-containing alkyl group. This slow initiation may be further hindered by the formation of alkyl-bridged dinuclear complexes as shown in Scheme 2, which should be more stable for methyl bridges [9] compared to ethyl or isobutyl bridges. Similar activation with 10-20 equivalents of Et_2Zn or $^nBu_2Mg$ instead of AlR_3 do not result in any activity. Addition of just one equivalent of Al^iBu_3 to the inactive Et_2Zn-activated solution does result in at least some

trimerisation activity. Thus, ZnR_2 or MgR_2 may be able to alkylate the chromium triflate complexes but cannot generate the apparently required dialkyl cationic complexes for catalysis.

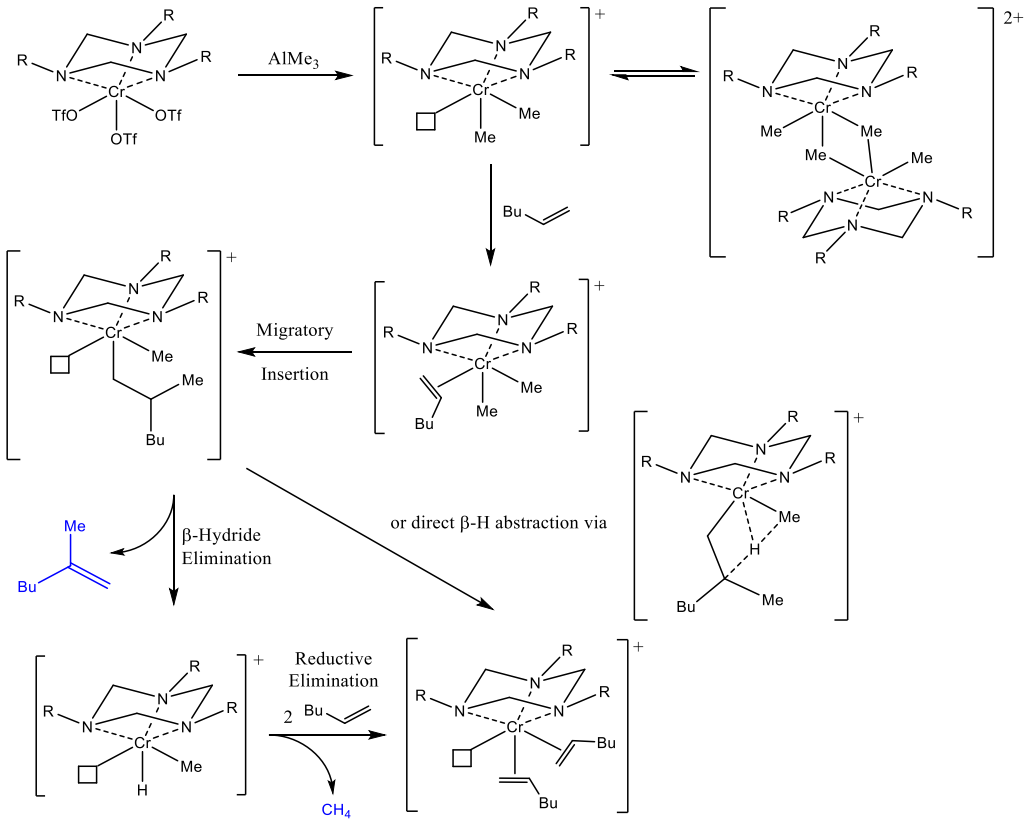

Scheme 2. Proposed activation mechanism

In order to assess the differences between aluminium alkyl activators, equal 1g portions of 0.5w% solutions of the most soluble complex **4c** in o-difluorobenzene are added to mixtures of about 110 eq AlR_3 (R= Me, Et, ^{i}Bu) in about 600 mg 1-hexene and followed by NMR. The larger than required excess of AlR_3 was used to ensure that there is no significant change in aluminium alkyl species by alkyl exchange reactions during activation (see later). There is a striking difference in the behaviours of the three activators. Figures 3 show the drop in 1-hexene and formation of trimers as well as hexene isomers.

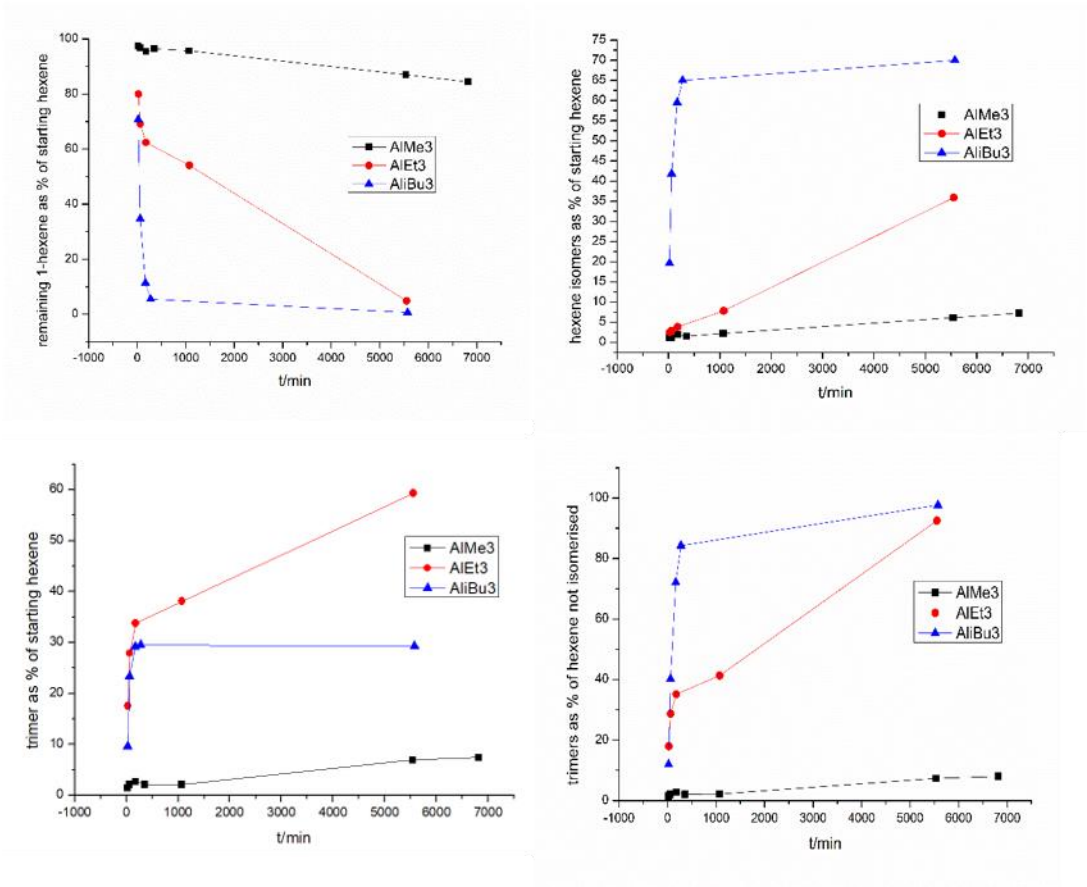

Figure 3. Comparing the reaction profile using $AlMe_3$, $AlEt_3$ and Al^iBu_3 with **4c**. Loss of 1-hexene (top left), formation of hexene isomers (top right) and formation of trimers (bottom left) as % of starting hexene or as % of hexene not isomerised (bottom right).

In each case the selectivity of these catalysts is inferior to their $R_3TACCrCl_3$/DMMAO analogues. While the oligomerisation selectivity (the proportion of trimer formed relative to other oligomers) remains extremely high at >99 mol%, as measured by GC-MS/FID, a far higher incidence of isomerisation is observed especially at low 1-hexene concentration leading to internal hexenes. We propose that this side reaction proceeds *via* a π-allyl complex mechanism, Scheme 3. This mechanism aligns well with that of metallacyclic trimerisation because of the matching Cr^I/Cr^{III} redox cycle proposed for both. The Cr^I-olefin adduct is also proposed as an accessible intermediate for both catalyst cycles, such that inter-conversion between reaction pathways would be expected.

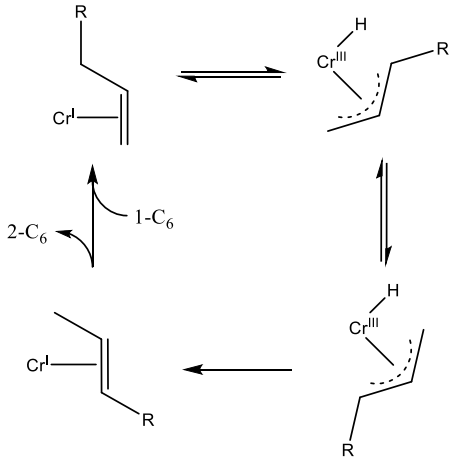

Scheme 3. Possible mechanism for olefin isomerisation via allyl complexes.

It is hypothesised that the greater propensity of $R_3TACCr(OTf)_3$ based catalysts to isomerise 1-hexene results from the presence of a different counter-ion. Several factors (catalyst dilution, 1-hexene equivalents, ligand bulk) significantly influence the ratio of trimerisation to isomerisation. This is attributed to the availability of the Cr^I-olefin adduct, as it is assumed that once a second olefin has co-ordinated to the chromium centre trimerisation becomes by far the more favoured process. Thus, reducing the 1-hexene concentration leads to an increase of isomerisation activity. Thus, isomerisation increases towards the end of trimerisation when the monomer concentration becomes low. Unfortunately, this competing reactivity hinders us from studying trimerisation at the initial stages at low olefin to Cr ratio where only isomerisation activity can be observed.

The relative isomerisation activity also depends greatly on the activating AlR_3. While activation with $AlMe_3$ gives only little isomerisation (<10%) at high enough olefin concentration (>1000 eq.), activation with Al^iBu_3 leads to more isomerisation than trimerisation. $AlEt_3$ gives fast activation with mainly trimerisation but more significant isomerisation (about 3:1). We found that optimal activation can be achieved by mixing some $AlMe_3$ with $AlEt_3$ or Al^iBu_3 leading to both fast activation and slow isomerisation. The use of mainly $AlEt_3$ also represents the most cost efficient reagent and therefore maximises the economic feasibility of this system relative to MAO based procedures.

Once $AlEt_3$ was identified as the preferred activating agent the equivalents required for complete activation of the catalyst were optimised. It was found that just four equivalents relative to the pre-catalyst were required for the formation of active catalyst. The use of smaller quantities still resulted in a colour change from blue to green, which is associated with alkylation of the chromium, but did not produce an active species. Therefore, the implication is that four equivalents are required to completely abstract triflate from the chromium and incorporate them into a weakly co-ordinating anion. Based on the demonstrated importance of a 3:4 ratio of triflate units to $AlEt_3$ in forming the counter-ion, its structure can be proposed, Scheme 4, which would be the simplest anion with all-four-coordinated aluminium and all-dimetallated triflate.

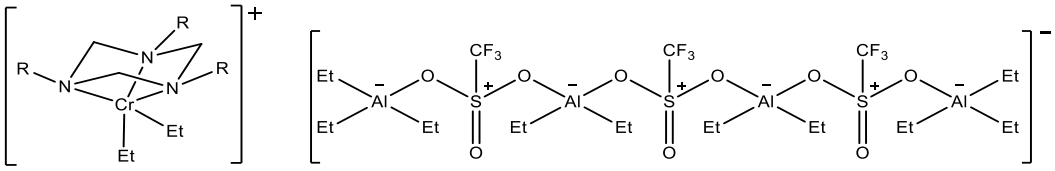

Scheme 4. The proposed structure of the activated catalyst and its counter-ion. Formal charges have been included at their respective positions within the counter-ion in order to clarify the overall charge.

This counter anion will likely weakly bind to the cationic chromium complexes. Bulkier R groups adjacent to a potential S=O binding site or alternative binding through the Al-R group similar to MAO may explain the isomerisation dependence on the type of AlR_3 used. Thus, the choice of the AlR_3 will influence the binding capability of the counter anion and ^{i}Bu based anions should be less coordinating than Me based anions. Thus, it can be hypothesised that a more weakly coordinating anion leads to more isomerisation. Use of a mixture of $AlMe_3$ and either $AlEt_3$ or $Al^{i}Bu_3$ would retain the strongest donor site of an $AlMe_3$ based anion while still showing fast activation as for $AlEt_3$ or $Al^{i}Bu_3$. Indeed, 2:1 mixtures of $AlEt_3$ or $Al^{i}Bu_3$ and $AlMe_3$ give fast activation and less than 25% isomerisation as shown in Figure 4.

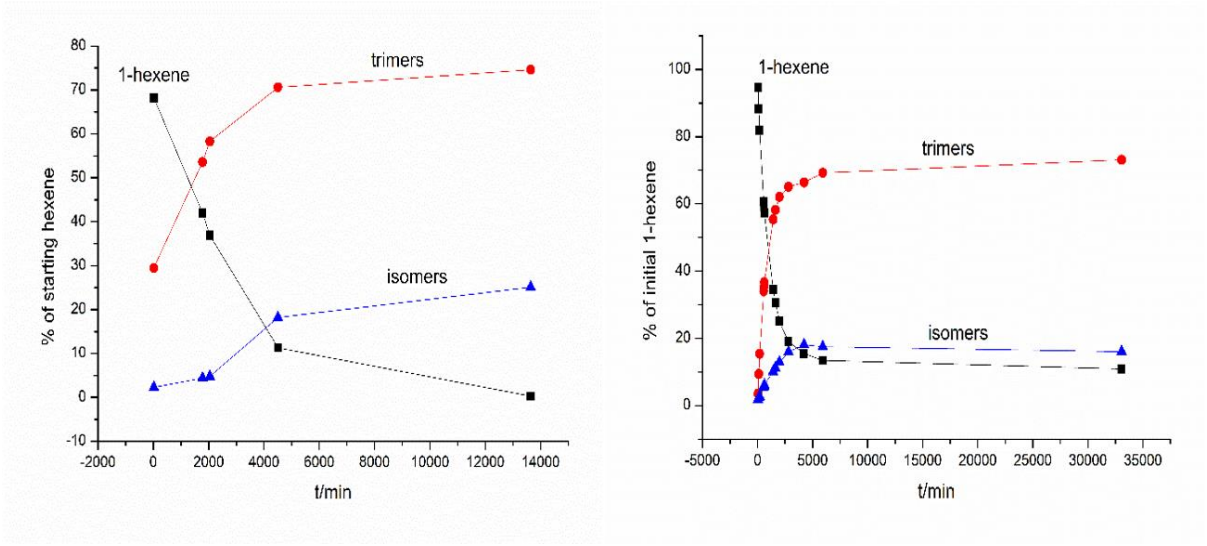

Figure 4. Reaction profile using Et_2AlMe (left) and $^{i}Bu_2AlMe$ (right) as activator for **4c**.

Under optimised conditions about 1000eq of trimerised olefin per chromium can be achieved with less than 10% isomerisation. The distribution of isomers in the trimer was determined by ^{13}C NMR as described before [10] and is found to be very similar between **1**/DMMAO and **4**/AlR_3 and depends much more on the N-substituent. Thus, the changing counter anion does not influence the isomer distribution very much.

Table 3. The main regioisomers produced on trimerisation of 1-hexene with either **1**/DMMAO or **4**/AlR_3 as catalyst (average over several runs). Structure of the isomers shown to the right [10].

	Regioisomer Abundance (%)							
Cat.	A	A’	B	B’	C	D	D’	E
4a	24	18	24	9	6	14	2	4
4b	37	6	5	5	9	18	4	6
1c	33	10	7	8	2	16	4	10
4c	34	10	8	7	4	17	3	7
1d	23	8	15	12	1	22	4	12
4d	20	9	14	9	0	24	4	13

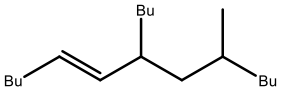

A (SS/RR), A' (SR/RS)

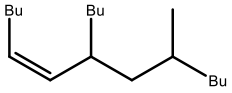

B (SR/RS), B' (SS/RR)

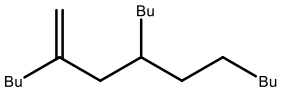

C

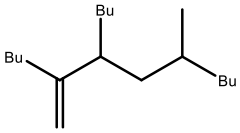

D (SS/RR), D' (SR/RS)

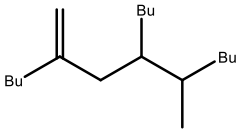

E (SS/RR), E' (SR/RS)

3.3 Analysis of the Activation Mechanism

Having established a catalyst capable of 1-hexene trimerisation at far lower aluminium alkyl loading than previous systems it was possible to perform the catalysis on a larger scale in order to investigate the activation products. With the use of 1 gram of catalyst, as opposed to 5 mg typically, activated with $AlMe_3$ and just six equivalents of 1-hexene it was possible to produce a product sample highly concentrated in the activation products. The proposed catalyst activation mechanism for olefin trimerisation has been expanded and adapted in Scheme 2 based on previous proposals relating to ethylene trimerisation.

The sample produced was analysed with the use of GC-MS/FID in an attempt to identify 2-methyl-1-hexene as a side product and provide evidence to support the proposed mechanism. However, analysis of the products in this manner indicated a range of side-products formed during activation. These could be identified by comparison of the corresponding fragmentation pattern to the NIST database, Figure 5. The key products were then confirmed with use of reference compounds and correlation of retention time under the same conditions, Figure 6. As a result, the presence of large quantities of C_6 and C_7 alcohols within the product mix was confirmed alongside 2-methyl-1-hexene.

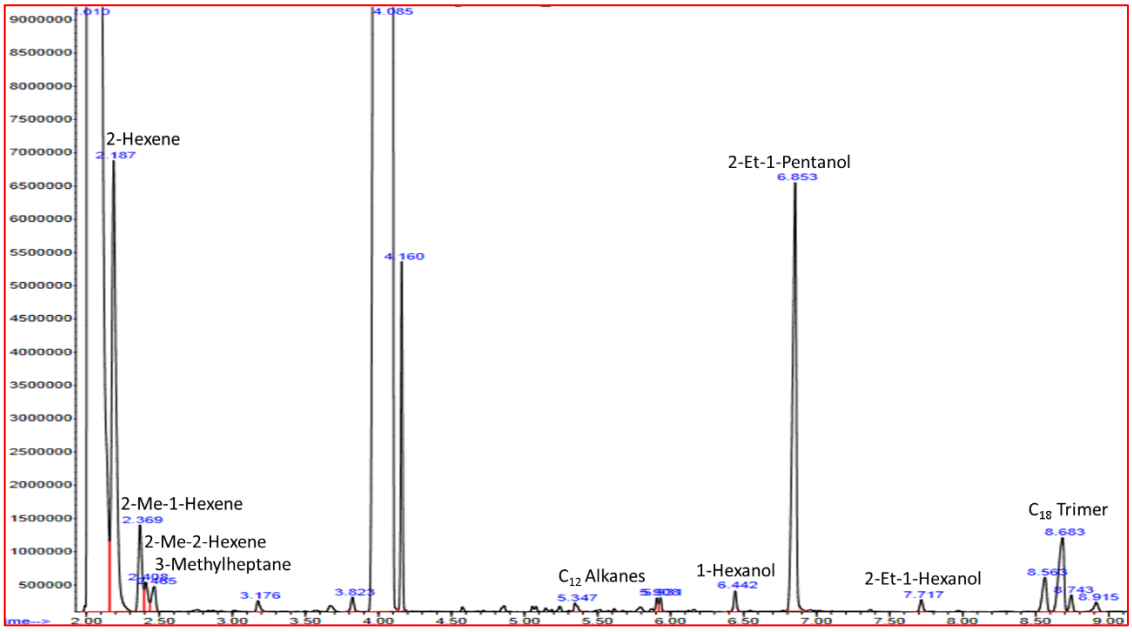

Figure 5. The products detected by GC-MS/FID on reaction of 6 equivalents of 1-hexene with $AlMe_3$ activated **4a.** The unlabelled peaks (2.010, 3.176, 3.823, 4.065 and 4.160) are derived from the *o*-$C_6H_4F_2$/pentane solvent and impurities within it, as determined by the control.

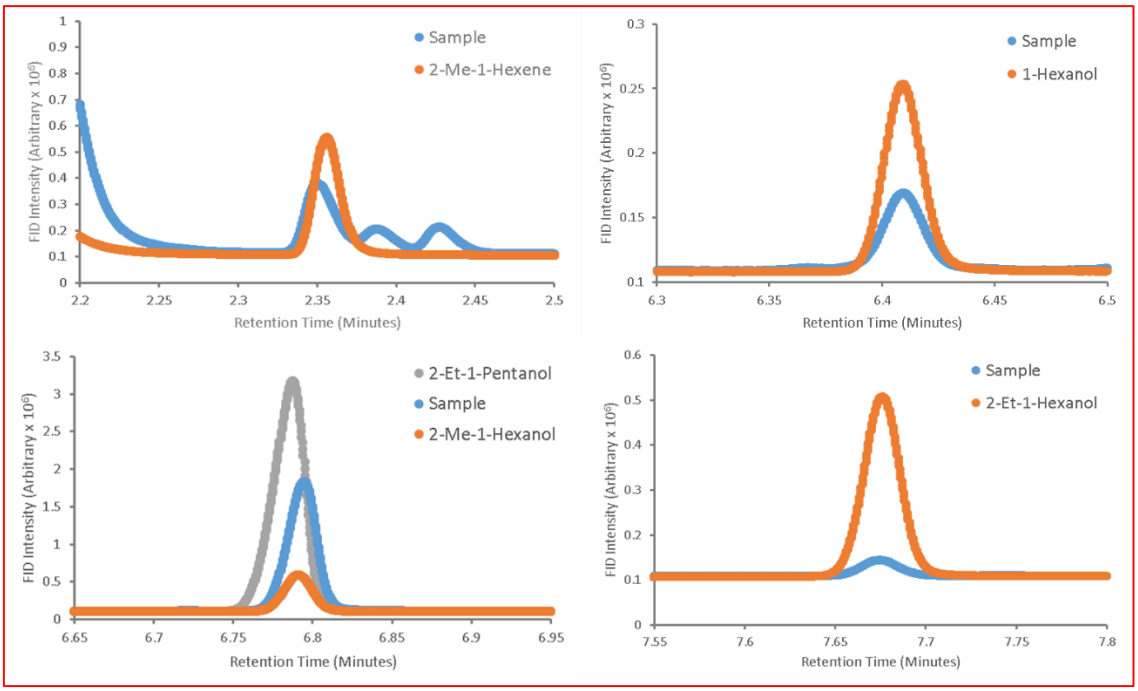

Figure 6. Correlation of retention times between reference compounds and the products of activation. 2-Hexene and the trimeric products were correlated with typical product samples within which these species are present in high abundance.

The key observation is that 2-methyl-1-hexene is formed as an activation product, which for the first time confirms the formation of the side product predicted by the mechanism originally proposed. The presence of its more stable isomerisation product 2-methyl-2-hexene is also not surprising under conditions with isomerisation activity. In contrast, the formation of several alcoholic species and 3-methylheptane was not predicted and the alcohols at least must form during exposure of the product

mix to oxygen after the reaction is complete. Analysis of the GC-FID spectrum allowed quantification of the various products and in turn the number of equivalents of 1-hexene converted to each could be calculated, Table 4. The observation of 1.7 eq. of 2-methyl-1-hexanol indicates significant alkyl exchange between chromium and $AlMe_3$ before β-H abstraction leading to more than just one insertion reaction of 1-hexene into the Cr-Me bond. 1-Hexanol could be explained by β-hydride elimination to coordinated 1-hexene rather than the methyl group leading to a Cr-hexyl group which can exchange to aluminium followed by oxidative workup to the alcohol. Small amounts of 3-methylheptane (and 2-ethyl-1-hexanol) may be due to ethyl impurities in the $AlMe_3$ or the product of C-C reductive elimination of the $[LCrMe(2\text{-methyl-1-hexyl})]^+$ intermediate.

Table 4. Products detected by GC after conversion of 6 eq. of 1-hexene

Activation Product	1-Hexene Equivalents Converted
2-Hexene	2.8
2-Methyl-1-Hexene	0.3
2-Methyl-2-Hexene	0.2
3-Methylheptane	0.1
C_{12} Alkanes	0.1
1-Hexanol	0.1
2-Methyl-1-Hexanol	1.7
2-Ethyl-1-Hexanol	< 0.1
C_{18} Trimer	0.9

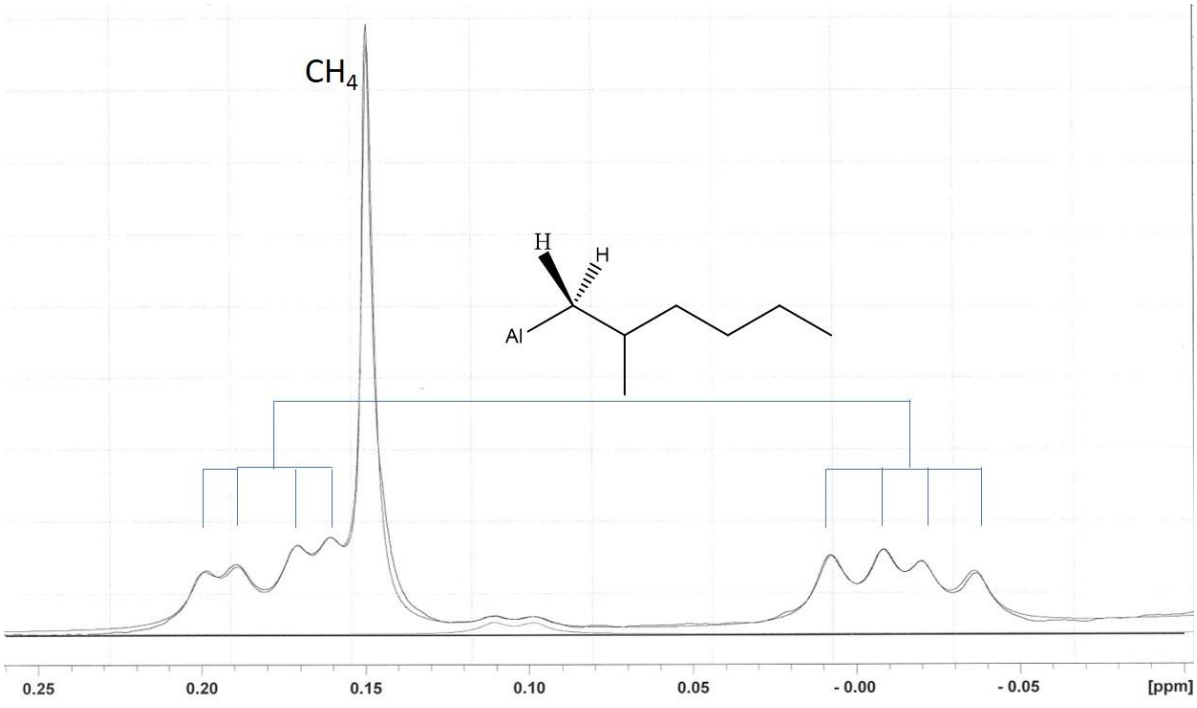

Figure 7. Additional Al-CH_2 ^1H NMR signal observed during of 1-hexene trimerisation with $AlMe_3$ activation

The processes during activation and deactivation can also be observed by NMR during trimerisation with **4c** in o-difluorobenzene and different AlR_3 described in 3.2. The region below 0.6 ppm in ^1H NMR shows signals for the α-hydrogens in AlR_3 and methane at 0.15 ppm in the case of $AlMe_3$ activation. Integration of the methane signal corresponds to a slightly more than one equivalent per chromium – as some methane may be lost during initial sample preparation and to the gas phase above the solution it is likely that more than one equivalent of methane is produced. Besides this methane signal and a large signal for $AlMe_3$ at –0.30 ppm a characteristic pair of two doublets of doublets is observed at +0.179 and –0.013 ppm with coupling constants of 5.1 + 14.0 and 7.9 + 14.0 Hz, respectively, as shown in Figure 7. This can be assigned to the two diastereotopic protons of a CH_2 group adjacent to a chiral centre. It shows ^1J coupling to ^{13}C at 21.7 ppm (HSQC) and $^{2/3}J$ coupling to 23.8, 30.3 and 41.8 ppm (HMBC) matching well the previously reported signals found for Me_2Al(2-methyl-1-hexyl) in benzene [36]. This signal grows rapidly in the early stages of the catalysis and increases only little later on reaching about 6 equivalents per chromium. This signal dominates all other Al-R signals observed in small amounts around 0.1 ppm. Opening the NMR tube to air at the end of the catalysis results in NMR signals for Al-OR groups around 3.5 ppm. Hydrolysis and distillation of all volatiles gives an o-difluorobenzene solution containing the remaining 1-hexene other volatile olefins and alcohols. The other olefins correspond to about 5% hexene isomers, about 3 equivalents of 2-methyl-1-hexene per chromium and a small amount of a more symmetrical vinylidene (possibly 2-ethyl-1-pentene) identified by their olefinic ^1H signals at 4.68+4.66 ppm and 4.69ppm, respectively, as well as their coupled ^{13}C signals (HSQC) at 110.3 and 106.9, respectively. The alcohols are mainly methanol at 3.35 ppm (s) and 2-methyl-1-hexanol [37] at 3.44dd (J= 5.6 and 10.3 Hz) and 3.35dd (6.7 and 10.3 Hz) besides a small amount of linear alcohol at 3.55t (J=6.6 Hz, likely 1-hexanol). These observations clearly show that the catalyst is activated with $AlMe_3$ by multiple 1-hexene insertions into Cr-Me bonds followed H-transfers before finally reducing to chromium(I) as shown in Scheme 5.

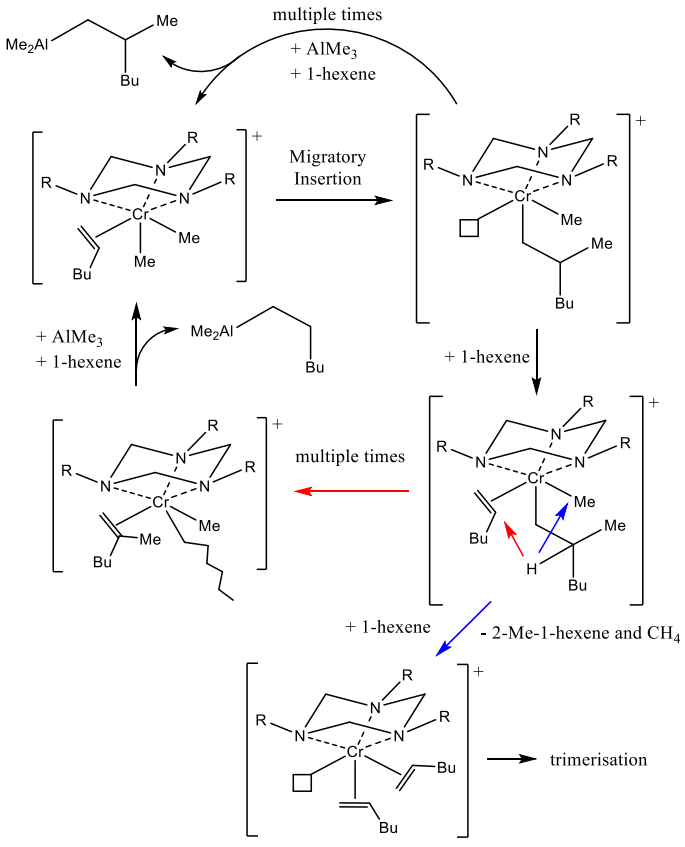

Scheme 5. Proposed mechanism of multiple activation via alkyl exchange with $AlMe_3$.

Activation with $AlEt_3$ or Al^iBu_3 does not require 1-hexene insertion prior to β-H abstraction as both have already β-hydrogen atoms. However, insertion into and β-hydrogen transfer to coordinated 1-hexene could still occur.

Activation with Al^iBu_3 quickly produces several equivalents of isobutene per chromium detectable at 4.63s (2H) and 1.65s (6H) growing more slowly but continuously during trimerisation reaching 90 equivalents per chromium for a sample activated with 100 eq of Al^iBu_3. At the same time a nearly equal amount of the initial Al-^{i}Bu observed at doublet at 0.30ppm in 1H NMR is converted into a triplet signal at 0.45ppm identified as Al-hexyl through its ^{13}C NMR signals observed by HSQC (13 ppm) and HMBC (26 and 36 ppm) matching the signals observed before for $^iBu_2$Al-hexyl [27]. Thus, the initial Al^iBu_3 is converted to hexyl rich AlR_3 during trimerisation especially when smaller excess Al^iBu_3 per chromium is used for activation.

Activation with 120 eq of $AlEt_3$ leads to detectable ethane (0.81ppm (^1H) and 7.2ppm (^{13}C) by HSQC) and some of the Al-Et signal observed as quartet at 0.36 ppm (^{13}C at 1.3 ppm (HSQC) and 9.1 ppm (HMBC)) is converted into an unidentified triplet at 0.17 ppm (^{13}C at 16 ppm (HSQC) and 32 and 39 ppm (HMBC)) as well as additional Al-R under the 0.36 ppm signal of Al-Et detectable by HSQC (7-11 ppm)/HMBC (26, 29, 36 ppm) which could include Al-hexyl as for Al^iBu_3 activation. After hydrolysis at the end of one catalysis run all room temperature volatiles at high vacuum were collected in a liquid nitrogen trap and analysed by NMR. It shows the expected solvent, remaining 1-hexene and isomerised hexenes but also a small amount of vinylidene at 4.689ttd (J=2.2+1.6+1.0 Hz) + 4.678ttd (1.7+0.6+1.0 Hz) coupling to ^{13}C at 108.1 ppm (HSQC) and 152.4, 37 and 29 ppm (HMBC) which could be assigned to 2-ethyl-1-hexene as the product of ethyl insertion into 1-hexene and subsequent elimination. The quantity of this product would correspond to about 3 equivalents per chromium. Thus, multiple insertion and alkyl transfer to aluminium seems to occur also for $AlEt_3$ and Al^iBu_3 activation.

Activation with a 2:1 mixture of Al^iBu_3 or $AlEt_3$ and $AlMe_3$ leads to fast formation of methane and isobutene in excess amounts as observed with single AlR_3 activation. Any ethylene that must be formed with $AlEt_3$ activation is likely incorporated in a mixture of isomeric co-trimers with 1-hexene and could not be identified.

Careful NMR observation also allows a study of ligand transfer to aluminium as a major decomposition pathway. During catalysis, additional signals shown in Figure 8 are observed in the otherwise empty region of 2.5-4.5 ppm in ^1H NMR. These signals include the characteristic pair of doublets previously observed and identified as the ring hydrogens coordinated to AlR_2^+ [7]. A third doublet of double intensity is also observed for the α-CH_2 of the N-substituent. The small but significant differences in the chemical shifts between different R groups indicate that they are still coordinated to this aluminium complex. When **4** is activated with only a minimum amount of AlR_3 needed these signals appear as complex signals of several overlapping doublets due to the formation of complexes with mixed alkyl groups due to the alkyl exchange reaction. When trimerisation has ceased after a few days, the integral of these signals correspond to 30-70% of the initial complex used. Thus, this is a major decomposition route but other inactive chromium complexes must also be formed. Irreversible decomposition occurs when all 1-hexene has been used up at low substrate loading as addition of new 1-hexene does not lead to further catalysis. However, if insufficient amounts (< 4 eq) of AlR_3 are added to start trimerisation, catalysis can be started by later addition of a few more equivalents AlR_3 even after several hours of inactivity. Thus, decomposition does not seem to occur before trimerisation starts.

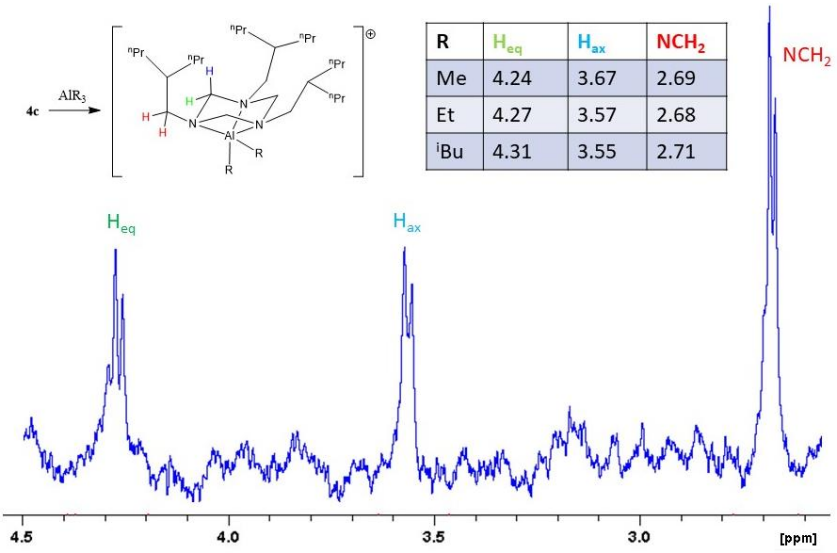

R	H_{eq}	H_{ax}	NCH_2
Me	4.24	3.67	2.69
Et	4.27	3.57	2.68
^{i}Bu	4.31	3.55	2.71

Figure 8. ^{1}H NMR signals observed for the LAl decomposition products during 1-hexene trimerisation with **4c**. The spectrum shown is for R=Et, the chemical shifts in ppm observed for the doublets are shown in the table.

3.4. Electrospray MS Studies

The proposed catalytic cycle involves mainly cationic chromium species. Thus, electrospray mass spectrometry (ESIMS) should be an ideal method to observe these intermediates. When we tried to observe MAO-activated solutions, we found that in our hands the large excess of MAO led to fast blocking of the thin PEEK or even steel tubing leading from a glovebox to the MS instrument, presumable by hydrolysis, despite thorough drying in an oven and under vacuum. This problem was much less pronounced with our new triflate/AlR_3 catalyst system. The much lower AlR_3 concentration allowed us to observe MS spectra for about 2 hours before the tube was blocked.

The reaction was split into two key stages. Firstly, the activation of the pre-catalyst was explored by excluding 1-hexene and simply adding the $AlMe_3$ activator (20 equivalents) to the pre-catalyst in the presence of the *o*-difluorobenzene solvent. For the MS studies, the most soluble complex $(^{i}Bu_2CH)_3TACCr(OTf)_3$ **4d** was used to avoid solubility problems especially after addition of large amounts of olefin. A sample of the solution was then taken one minute after addition and injected into the mass spectrometer while under argon. In this way, the sample could be analysed immediately and the ionic species present at this stage of the reaction readily detected.

The mass spectrum observed for this sample was remarkably clean, with just one set of peaks prominent. The distinctive isotope pattern (Figure 9) matched that expected for $[((^{i}Bu_2CH)_3TAC)CrMe_2]^{+}$, the alkylation product predicted by the metallacyclic mechanism. A smaller signal (about 10%) of $[((^{i}Bu_2CH)_3TAC)CrMe(OTf)]^{+}$ can also be detected at m/z = 681.4029 (calcd 681.4177) as an intermediate of this activation process. Identification of $[((^{i}Bu_2CH)_3TAC)CrMe_2]^{+}$ lends considerable support to the initiation of the metallacyclic mechanism and agrees with the EPR spectroscopy carried out by Bercaw *et al*..[16]

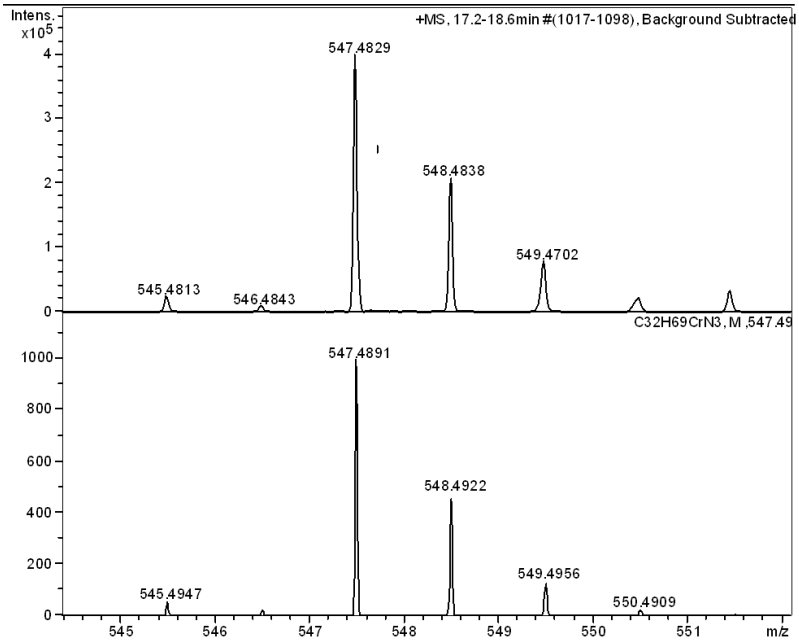

Figure 9. The observed (top) and simulated (bottom) m/z peaks corresponding to $[((^{i}Bu_2CH)_3TAC)CrMe_2]^+$.

After addition of 1-hexene (either 450 or 5000 equivalents per Cr) to a portion of the same mixture another MS sample was taken. Now there were considerably more signals present in the spectrum, suggesting a multitude of species are formed on addition of 1-hexene. While many of these signals could not be assigned, the major species present and several minor species were found to correlate with those expected for the intermediates proposed in Scheme 5. The previously dominating signal for $[((^{i}Bu_2CH)_3TAC)CrMe_2]^+$ is still present throughout the 2 hours of the MS experiments supporting the slow activation with $AlMe_3$ observed by NMR. Indeed, this slow activation provides relatively constant conditions of trimerisation throughout the experiment making observed intensities approximately comparable. In addition, ions corresponding mainly to species of the composition $[((^{i}Bu_2CH)_3TAC)Cr(C_6H_{12})_n]^+$ (n=0-4) are observed. In MS, we can only detect the total mass and several different species of the same composition as shown in Scheme 6 could be responsible for the observed cations.

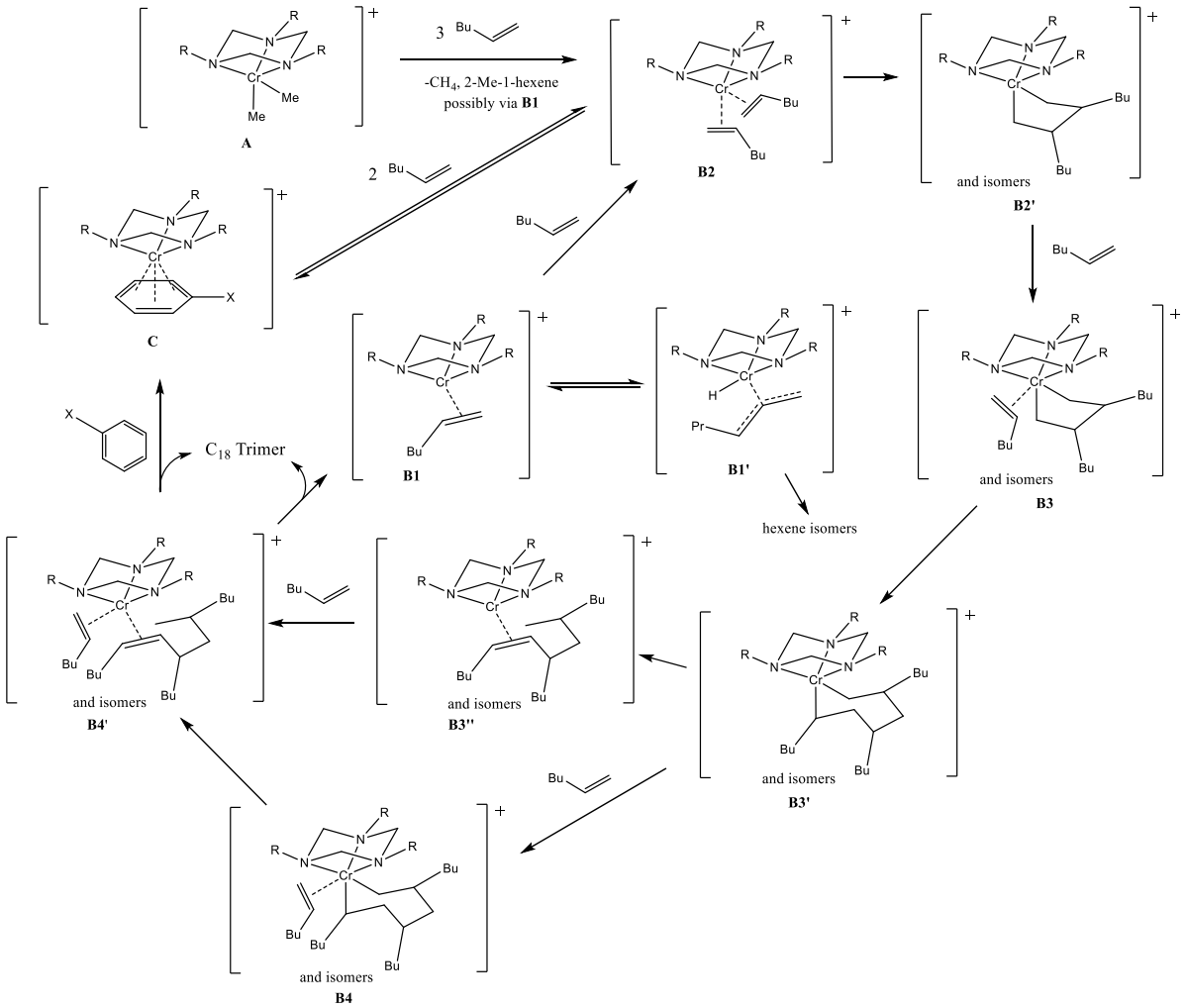

Scheme 6. The proposed intermediates of selective 1-hexene trimerisation based on mass spectrometric observation of cations of $LCrMe_2$ (**A**), LCr(1-hexene) (**B1** and **B1'**), LCr(1-hexene)$_2$ (**B2** and **B2'**), LCr(1-hexene)$_3$ (**B3**, **B3'** and **B3''**), LCr(1-hexene)$_4$ (**B4** and **B4'**), and LCr(arene) (**C**)

Table 5. The proposed intermediates that were found to have corresponding peaks in the mass spectrum during reaction with 1-hexene.

Catalytic Intermediate	Observed m/z	Calculated m/z	rel Intensity 450 eq 1-hexene	rel Intensity 5000 eq 1-hexene
$[(({}^{i}Bu_2CH)_3TAC)Cr]^+$	517.4338	517.4422	100	100
$[(({}^{i}Bu_2CH)_3TAC)Cr(C_6H_{12})]^+$	601.5198	601.5361	20	-
$[(({}^{i}Bu_2CH)_3TAC)Cr(C_6H_{12})_2]^+$	685.6142	685.6300	9	8
$[(({}^{i}Bu_2CH)_3TAC)Cr(C_6H_{12})_3]^+$	769.7140	769.7239	9	45
$[(({}^{i}Bu_2CH)_3TAC)Cr(C_6H_{12})_4]^+$	853.7976	853.8179	3	3
$[(({}^{i}Bu_2CH)_3TAC)Cr(C_7H_{14})]^+$	615.5401	615.5518	60	-
$[(({}^{i}Bu_2CH)_3TAC)Cr(C_{13}H_{26})]^+$	699.6275	699.6457	9	-

The relative intensities of the peaks shown in Table 5 are likely to be indicative of the relative concentrations. Observation of $[(({}^{i}Bu_2CH)_3TAC)Cr]^+$ is highly significant because it confirms that chromium(I) with coordinated ligand is present. While a naked species like this is unlikely in the solution during catalysis, it may indicate the presence of Cr(I) complexes with weakly coordinated

neutral ligands that can be lost in the gas phase activation within the MS instrument. The observation of significant amounts of complex cations made up from two and three olefins supports the presence of metallacyclopentane and –heptane species as expected from the proposed catalytic cycle with increased amounts of metallocycloheptane at higher monomer concentration. The observation of cations made up of four olefins is surprising as no tetramerisation is detectable by GC in any of these systems. Thus, this ion must be made up of coordinated monomer plus trimer either before (**B4**) or after β-H abstraction (**B4'**) rather than a metallacyclononane. Observation of a significant amount of cations containing only one olefin at relatively low monomer loading while not at high monomer concentration may be due to formation of Cr(III) allyl hydride complexes (**B1'**) proposed as intermediates of the olefin isomerisation side reaction rather than a Cr(I) complex (**B1**). This explanation would also agree with the observation of hardly any isomerisation during catalysis with 5000 eq. olefin, significant isomerisation at 450 eq and almost exclusive isomerisation at fewer than 100 eq of olefins.

At low olefin concentration, two other peaks can be identified corresponding to complexes containing C_7H_{14} and 1-hexene+C_7H_{14}. This would correspond to ions formed from inclusion of 2-methyl-hexene (C_7H_{14}) which is formed as initiation product identified by GCMS (see above). As above, the C_7H_{14} complex may be more likely present as the allyl hydride Cr(III)-complex rather than as mono-olefin-Cr(I) complex. Either way, the observation of these as significant cations confirms 2-methyl-hexene as initiation product.

Identification of these 1-hexene containing intermediates was confirmed by addition of 500 eq. of 1-octene to another portion of the same $AlMe_3$ activated catalyst. The analogous cationic species in approximately the same proportions were detected as shown in Table 6. No cation corresponding to five olefins was detected in either experiment. Thus, co-trimerisation of trimer product with two monomers can be excluded within detection limits and an initially formed complex **B4'** leads to olefin substitution **B1** to **B2** before oxidative cyclisation can occur.

Table 6. The proposed intermediates that were found to have corresponding peaks in the mass spectrum during reaction with 1-octene.

Catalytic Intermediate	Observed m/z	Calculated m/z	rel Intensity 500 eq 1-octene
$[(({}^{i}Bu_2CH)_3TAC)Cr]^+$	517.4338	517.4422	100
$[(({}^{i}Bu_2CH)_3TAC)Cr(C_8H_{16})]^+$	629.5528	629.5674	14
$[(({}^{i}Bu_2CH)_3TAC)Cr(C_8H_{16})_2]^+$	741.6804	741.6826	9
$[(({}^{i}Bu_2CH)_3TAC)Cr(C_8H_{16})_3]^+$	853.7997	853.8179	7
$[(({}^{i}Bu_2CH)_3TAC)Cr(C_8H_{16})_4]^+$	965.9260	965.9431	1
$[(({}^{i}Bu_2CH)_3TAC)Cr(C_9H_{18})]^+$	643.5775	643.5831	170
$[(({}^{i}Bu_2CH)_3TAC)Cr(C_{17}H_{34})]^+$	755.5165	755.7083	22

The $AlMe_3$ activated solution with 450 eq 1-hexene was also tested for incorporation of other olefins. Addition of excess cyclopentene to a portion of this solution resulted in no detectable ions $[(({}^{i}Bu_2CH)_3TAC)Cr(cyclopentene)(C_6H_{12})_n]^+$. Thus, cyclopentene does not seem to bind or insert in any significant amount. Addition of 1,7-octadiene to another portion does result in a clear set of signals corresponding to $[(({}^{i}Bu_2CH)_3TAC)Cr(octadiene)]^+$ at m/z = 627.5366 (calcd. 627.5518) but no signal corresponding to a cation containing both octadiene and hexene. Thus, the octadiene can bind to Cr(I) and maybe oxidatively add to form a metallacyclopentane but seems to be incapable of inserting any 1-hexene. In a synthetic experiment no trimerisation was observed when 1,7-octadiene was added to 1-hexene before addition to activated catalyst and thus acts as catalyst poison.

Table 7. Arene complexes **C** detected with intensities relative to $[(({}^{i}Bu_2CH)_3TAC)Cr]^+$ (*toluene complex observed in sample with 5000 eq 1-hexene)

Catalytic Intermediate	Observed m/z	Calculated m/z	rel Intensity 500 eq 1-hexene
$[(({}^{i}Bu_2CH)_3TAC)Cr]^+$	517.4338	517.4422	100
$[(({}^{i}Bu_2CH)_3TAC)Cr(C_6H_4F_2)]^+$	631.4317	631.4703	2 (0*)
$[(({}^{i}Bu_2CH)_3TAC)Cr(C_6H_5F)]^+$	613.5379	613.4797	8
$[(({}^{i}Bu_2CH)_3TAC)Cr(C_6H_6)]^+$	595.3810	595.4892	1
$[(({}^{i}Bu_2CH)_3TAC)Cr(toluene)]^+$	609.4752	609.5048	4*
$[(({}^{i}Bu_2CH)_3TAC)Cr(p\text{-}xylene)]^+$	623.4041	623.5205	27
$[(({}^{i}Bu_2CH)_3TAC)Cr(cymene)]^+$	651.5089	651.5518	0.5

ESIMS also allows testing for the proposed arene complex **C** during the catalytic cycle. The $AlMe_3$ activated solution with 450 eq 1-hexene shows a signal for $[(({}^{i}Bu_2CH)_3TAC)Cr(C_6H_4F_2)]^+$, a Cr(I) complex with the o-difluorobenzene solvent. The same cation was not detected when the solution contained 5000 eq 1-hexene. Thus, large excess of olefin suppresses the presence of this cation and therefore also decomposition to inactive $[Cr(arene)_2]^+$ which was previously identified as a major decomposition product for benzene and toluene. Subsequently, about 20% of other arenes were added to the solution (thus, o-difluorobenzene was still in excess) to identify any other arene complexes as shown in Table 7. While this experiment is not fully quantitative, it shows the expected trend for more electron rich arenes to bind more strongly than o-difluorobenzene unless sterically hindered (cymene). The formation of these arene cations will likely be in competition with the catalytic cycle justifying o-difluorobenzene as the solvent of choice for faster trimerisation.

Overall, analysis of the cationic intermediates using mass spectrometry has provided direct evidence for the existence of metallacyclic intermediates for the first time. While chain growth via a possible Cossee-Arlman mechanism and olefin insertion into chromium dialkyl species has been previously ruled out by Bercaw's isotope studies, this MS study lends further evidence against chromium dialkyl cations which would have cations of the formula $[(({}^{i}Bu_2CH)_3TAC)Cr(olefin)_nH_2]^+$ which was not observed.

Apart from an investigation into co-catalysts carried out by McGuinness *et al*. [38] very little attention has been paid to the counter-ion during catalysis. While in some defined cases the structure of the counter-ion is evident due to the addition of an abstraction agent alongside the alkylating agent, in the case of $AlMe_3$ activation it is less clear.[39] The use of negative ion MS during the catalysis allowed insights into the species formed as the counter-ion after completion of the alkylation and abstraction steps.

At relatively low m/z values there were two significant peaks that corresponded to the expected anions containing only one aluminium atom. These were characterised as $[AlMe_3(OTf)]^-$ and $[AlMe_2(OTf)_2]^-$, Figure 10, of which the dimethyl species was by far the most abundant on comparison of peak intensities. This indicates that $AlMe_3$ units which abstract a triflate group are typically also involved in alkylation of the chromium. The considerable number of higher molecular weight products observed were therefore predicted to result from this initial product. The proposed counter-ion would also result from this same initial product, lending some support to its existence.

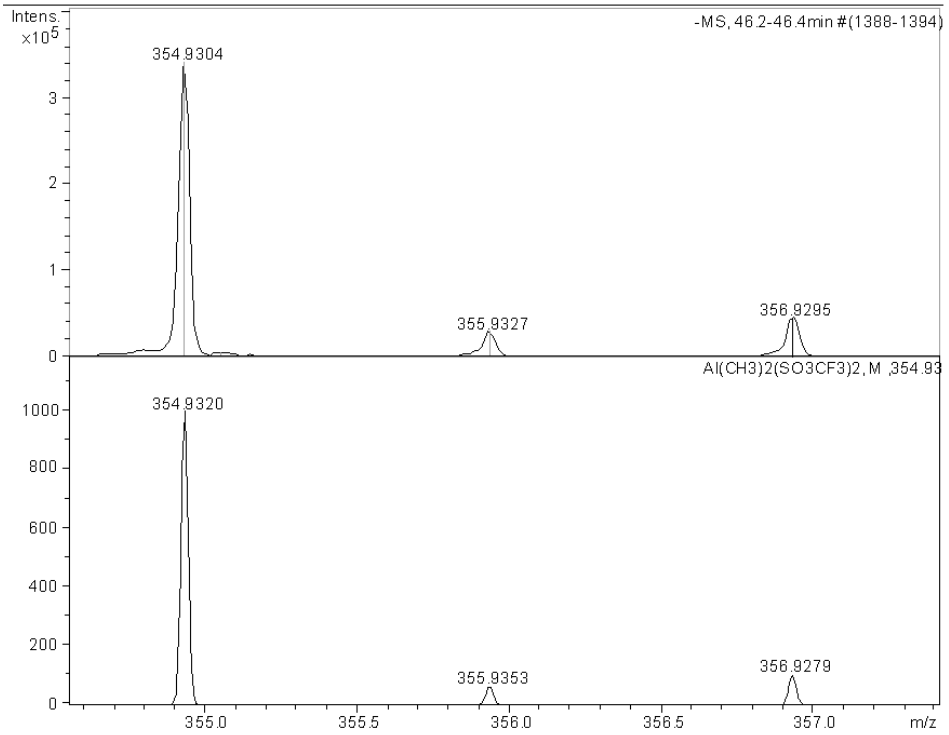

Figure 10. The observed (top) and calculated (bottom) m/z peaks corresponding to $[AlMe_2(OTf)_2]^-$.

Analysis of the higher molecular weight products showed that most contained two triflate groups, as would be expected from the higher abundance of $[AlMe_2(OTf)_2]^-$. Unfortunately, the products also corresponded to products containing increased levels of oxygen than would have been expected. This indicated that either oxygen or moisture had contaminated the highly reactive aluminium species to give far more products than expected. These could be identified as those shown in Chart 1, in each case the isotope pattern was observed as expected.

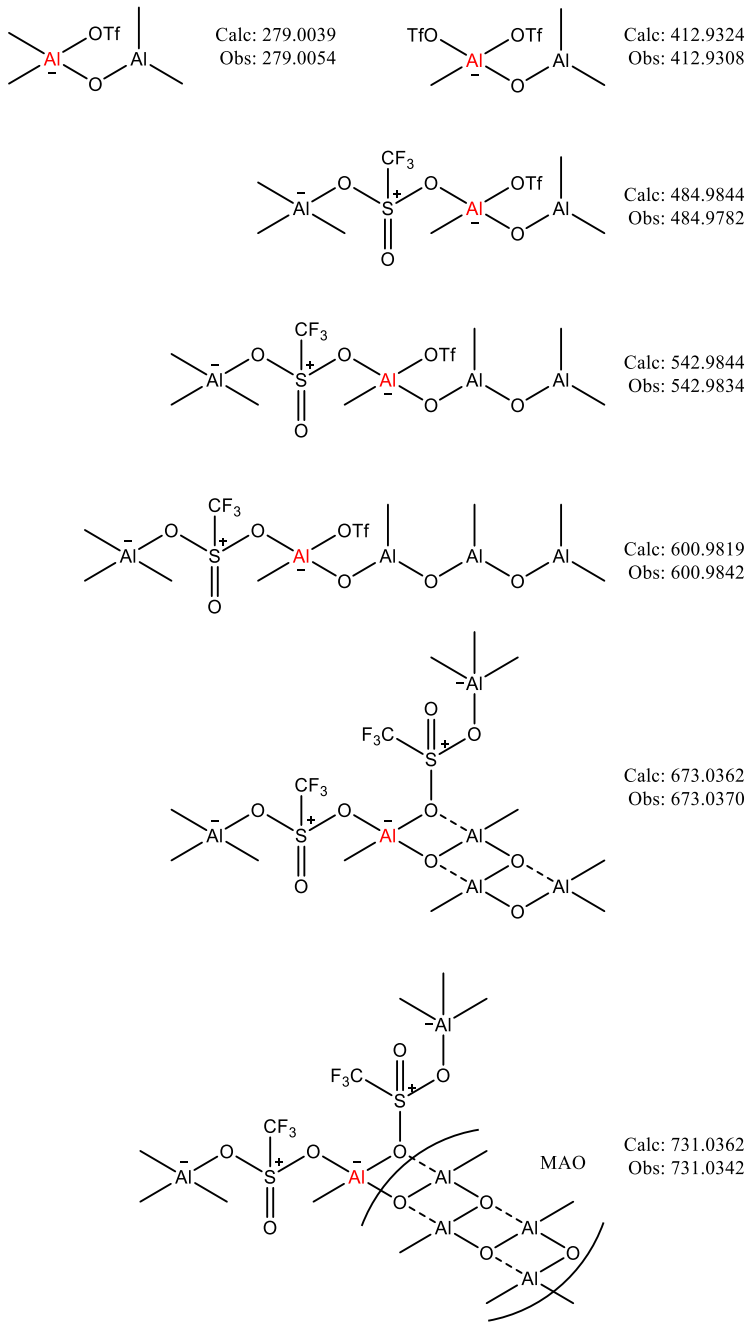

Chart 1. The anionic aluminium species detected. The aluminium that is carried forwards from the original product is shown in red.

It can be seen that the number of major products is determined by the growth of methylaluminoxane chains. This strongly indicates that moisture is the source of contamination, with no methoxy groups detected. Larger molecules are probably formed but remain unobserved due to increasingly poor solubility in *o*-$C_6H_4F_2$. With the aluminium species thought to act as a scavenger in all cases it appears that this may in fact be beneficial, with the counter-ion becoming more like the highly effective MAO in the presence of low concentrations of moisture. Therefore, this activation route appears highly effective as the potency of the catalyst is unlikely to be lost due to low level contamination, assuming the scavenger prevents the chromium from being affected.

Despite these complications it was still possible to observe that the triflate groups can indeed act as bridging ligands that incorporate a formally positive charge. Peak 484.98, for example, cannot be accounted for by any other logical arrangement of the atoms shown to be present by MS analysis. This lends considerable support to the proposed counter-ion under ideal conditions. With the presence of moisture confirmed, the spectra were checked for peaks corresponding to species in which hydroxy groups had been incorporated. This led to the discovery of two peaks that gave even stronger evidence in favour of the proposed anionic species, Chart 2, in both cases the expected isotope pattern was observed.

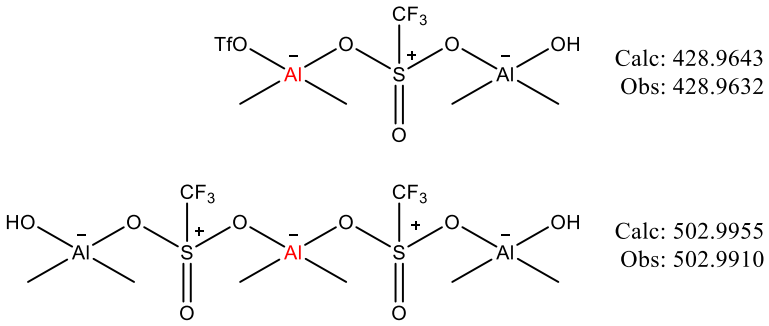

Chart 2. The two large anions detected that were shown to contain hydroxyl groups.

These two species, and especially the anion observed at 502.99, bear a striking resemblance to the proposed counter-ion. These products demonstrate that formally cationic triflate groups are able to bridge between anionic aluminium centres, producing large anions of diffuse charge suitable for catalysis. Observation of these species strongly supports the proposed structure of the counter-ion and allows speculation on the mechanism by which it is formed.

Unfortunately, under the conditions of this reaction a species containing a 4:3 ratio of aluminium to triflate could not be detected. This is likely as a result of the disruption caused by the presence of moisture. Further optimisation of the reaction conditions is required before a concerted attempt at detection of the counter-ion under ideal catalytic conditions can be made.

Following on from investigation of the side-products of activation and the proposed chain transfer chemistry, the spectra were also studied for evidence of the related aluminium species. As predicted, two significant signals were observed in the sample taken after addition of 1-hexene that corresponded with 2-methylhexyl aluminium species, Chart 3.

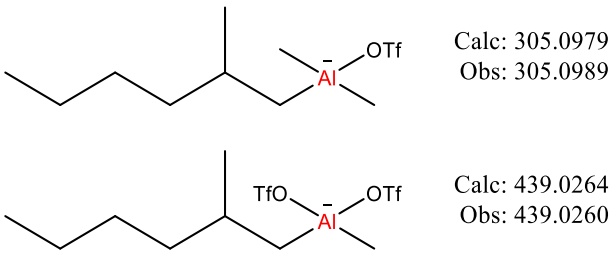

Chart 3. The two principal aluminium species containing 2-methylhexyl groups.

Observation of these two species confirms chain transfer reactions as the source of the greater than expected equivalents of 2-methylhexyl based side products. In addition to these major species, numerous additional anions containing the 2-methylhexyl group were observed as a result of partial oxidation. The two corresponding species in which a second methyl group had been substituted were also observed, indicating that chain transfer is a fairly favourable process even when sterically hindered. These results strongly support the proposed activation mechanism and provide firm evidence that the alcohol containing species result from aluminium complexes on work-up in air. Aluminium species corresponding to the two minor alcohols formed, hexanol and 2-ethylhexanol, were not observed but it follows that they are formed in the same manner.

Overall, analysis of the anion with mass spectrometry provided considerable support for the proposed counter-ion. Principally, the analysis allowed observation of species containing cationic triflates as bridging ligands between anionic aluminium units. As such, the connectivity and chemistry proposed to account for the formation of the counter-ion has been demonstrated experimentally, though unfortunately the species itself has not been observed. Observation of this chemistry allowed the proposal of a counter-ion formation mechanism that accounts for the observed requirement for four equivalents of $AlMe_3$. Further analysis also confirmed the existence of chain transfer reactions, strongly supporting the proposed activation mechanism.

4. Conclusion

We have described herein a range of novel catalysts capable of the trimerisation of α-olefins at high activities and a fraction of the cost of established MAO dependent systems. The catalysts can be synthesised *via* $Cr(THF)_3(OTf)_3$, the novel structure of which has been determined by X-ray crystallography, which allows access to a simple two-step catalyst synthesis. Optimisation of the catalyst activation has demonstrated that complete conversion to the active species can be achieved with just four equivalents of $AlEt_3$. Based on this ratio the structure of the weakly co-ordinating counter-ion has been proposed.

The cost effective and well defined nature of the process allowed large scale investigation of the activation mechanism. It was found that 2-methyl-1-hexene was formed after $AlMe_3$ activation as predicted previously by Köhn *et al*., providing considerable experimental evidence in support of the metallacyclic mechanism for olefin trimerisation.

The low aluminium alkyl content allowed us to observe electrospray mass spectrometry during catalysis and to identify many of the intermediates proposed by a metallacyclic mechanism. The observation of cations containing four olefin units while no tetramerisation is observed indicates the involvement of intermediates containing both the trimer and a monomer coordinated to chromium. We are currently exploring the possible implications for the mechanism by computational methods.

Acknowledgement

This research was jointly supported by LyondellBasell and the EPSRC (Alexander Coxon). This work was also supported by the Engineering and Physical Sciences Research Council EP/L016354/1 (Callum Heron).

Appendix A. Supplementary Data

CCDC **1969785**, **1969790**, **1969787**, **1969788**, **1969786**, **1969789**, **1969791** contain the supplementary crystallographic data for **3**, **$CrCl_3(THF)_3$**, **1a**, **1b**, **4a**, **4b** and $[Cr(H_2O)_6](OTf)_3 \cdot 3H_2O$, these data can be obtained free of charge via http://www.ccdc.cam.ac.uk/conts/retrieving.html,or from the Cambridge Crystallographic Data Centre, 12 Union Road, Cambridge CB2 1EZ, UK; fax: +44 1223-336-033; or e-mail: deposit@ccdc.cam.ac.uk.
Selected MS data, full isomer distribution of trimers, a picture and some crystal data for $[Cr(H_2O)_6](OTf)_3 \cdot 3H_2O$, and NMR spectra of ligand precursors and complexes **1c,d** and **4c,d** are provided as supplementary material.

References

[1] O. L. Sydora, Organometallics 38 (2019) 997-1010 and references therein

DOI: 10.1021/acs.organomet.8b00799

[2] K. A. Alferov, G. P. Belov, Y. Meng, Applied Catalysis A, General 542 (2017) 71–124

DOI: 10.1016/j.apcata.2017.05.014

[3] R. D. Köhn, A. G. N. Coxon, C. R. Hawkins, D. Smith, S. Mihan, K. Schuhen, M. Schiendorfer, G. Kociok-Köhn Polyhedron 84 (2014) 3–13

DOI: 10.1016/j.poly.2014.05.050

[4] R. D. Köhn, M. Haufe, S. Mihan, D. Lilge Chem. Commun. (2000) 1927–1928

DOI: 10.1039/b005842o

[5] A. Sattler, J. A. Labinger, J. E. Bercaw Organometallics 32 (2013) 6899−6902

DOI: 10.1021/om401098m

[6] T. E. Stennett, M. F. Haddow, D. F. Wass Organometallics 31 (2012) 6960−6965

DOI: 10.1021/om300739m

[7] R. D. Köhn, D. Smith, M. F. Mahon, M. Prinz, S. Mihan, G. Kociok-Köhn J. Organomet. Chem. 683 (2003) 200-208

DOI: 10.1016/S0022-328X(03)00634-X

[8] A. Sattler, D. C. Aluthge, J. R. Winkler, J. A. Labinger, J. E. Bercaw, ACS Catal. 6 (2016) 19−22
DOI: 10.1021/acscatal.5b02604

[9] R. D. Köhn, M. Haufe, G. Kociok-Köhn, S. Grimm, P. Wasserscheid, W. Keim Angew. Chem. Int. Ed. 39 (2000) 4337–4339

DOI: 10.1002/1521-3773(20001201)39:23<4337::AID-ANIE4337>3.0.CO;2-4

[10] A. G. N. Coxon, R. D. Köhn ACS Catal. 6 (2016) 3008−3016

DOI: 10.1021/acscatal.6b00542

[11] R. Manyik J. Catal. 47 (1977) 197– 209

DOI: 10.1016/0021-9517(77)90167-1

[12] J. R. Briggs, J. Chem. Soc., Chem. Commun. 11 (1989) 674– 675

DOI: 10.1039/c39890000674

[13] T. Agapie, S. J. Schofer, J. A. Labinger, J. E. Bercaw J. Am. Chem. Soc. 126 (2004) 1304-1305

DOI: 10.1021/ja038968t

[14] R. Arteaga-Müller, H. Tsurugi, T. Saito, M. Yanagawa, S. Oda, K. Mashima J. Am. Chem. Soc. 131 (2009) 5370-5371

DOI: 10.1021/ja8100837

[15] R. Emrich, O. Heinemann, P. W. Jolly, C. Krüger, G. P. J. Verhovnik Organometallics 16 (1997) 1511-1513

DOI: 10.1021/om961044c

[16] L. H. Do, J. A. Labinger, J. E. Bercaw ACS Catal. 3 (2013) 2582−2585

DOI: 10.1021/cs400778a

[17] J. S. McIndoe, K. L. Vikse J Mass Spectrom. 54 (2019) 466–479

DOI: 10.1002/jms.4359

[18] H. S. Zijlstra, M. Linnolahti, S. Collins, J. S. McIndoe Organometallics 36(2017) 1803−1809

DOI:10.1021/acs.organomet.7b00153

[19] R. D. Köhn, M. Haufe, G. Kociok-Köhn, M. Haufe J. Organomet. Chem. 501 (1995) 303-307

DOI: 10.1016/0022-328X(95)05701-P

[20] D. H. Grant, J. Chem. Educ. 72 (1995) 39-40

DOI: 10.1021/ed072p39

[21] C. Piguet, J. Chem. Educ. 74 (1997) 815-816

DOI: 10.1021/ed074p815

[22] IPDS (STOE Software 2.65, 1996)

[23] DENZO-SCALEPACK Z. Otwinowski and W. Minor, " Processing of X-ray Diffraction Data Collected in Oscillation Mode ", Methods in Enzymology, Volume 276: Macromolecular Crystallography, part A, p.307-326, 1997,C.W. Carter, Jr. & R. M. Sweet, Eds., Academic Press.

[24] CrysAlisPro 1.171.39.46 (Rigaku Oxford Diffraction, 2018)

[25] L. J. Farrugia, J. Appl. Cryst., 32 (1999) 837-838

DOI: 10.1107/S0021889899006020

[26] L. V. Parfenova, V. Z. Gabdrakhmanov, L. M. Khalilov, U. M. Dzhemilev, J. Organomet. Chem. 683 (2003) 200-208

DOI: 10.1016/j.jorganchem.2009.07.037

[27] L. V. Parfenova, S. V. Pechatkina, L. M. Khalilov, U. M. Dzhemilev, Russian Chemical Bulletin, 2005, vol. 54, # 2, p. 316 - 327]

DOI: 10.1007/s11172-005-0254-z

[28] C. J. H. Jacobsen, J.Villadsen, H. Weihe Inorg. Chem. 32 (1993) 5396-5397

DOI: 10.1021/ic00075a072

[29] C. K. Ryu, R. B. Lessard, D. Lynch, J. F. Endicott J. Phys. Chem. 93 (1989) 1752-1759

DOI: 10.1021/j100342a017

[30] M. E. M. Hamidi, J.-L. Pascal Polyhedron 13 (1994) 1787-1792

DOI: 10.1016/s0277-5387(00)80111-4

[31] C. R. J. Lepage, L. Mihichuk, D. G. Lee Can. J. Chem. 81 (2003) 75 – 80

DOI: 10.1139/v02-201

[32] C. Postmus, E. L. King J. Phys. Chem. 59 (1955) 1208–1216

DOI: 10.1021/j150534a007

[33] H. Taube, A. Scott Inorg. Chem. 10 (1971) 62-66

DOI: 10.1021/ic50095a013

[34] J. Y. Jeon, J. H. Park, D. S. Park, S. Y. Park, C. S. Lee, M. J. Go, J. Lee, B. Y. Lee Inorg. Chem. Commun. 44 (2014) 148-150

DOI:10.1016/j.inoche.2014.03.023

[35] F. A. Cotton, S. A. Duraj, G. L. Powell, W. J. Roth Inorg. Chim. Acta 113 (1986) 81-85

DOI:10.1016/S0020-1693(00)86863-2

[36] L. V. Parfenova , V. Z. Gabdrakhmanov, L. M. Khalilov, U. M. Dzhemilev, J. Organomet. Chem. 694, 2009, 3725-3731

DOI: 10.1016/j.jorganchem.2009.07.037

[37] L. V. Parfenova, T. V. Berestova, T. V. Tyumkina, P. V. Kovyazin, L. M. Khalilov, R. J. Whitby, U. M. Dzhemilev Tetrahedron: Asymmetry 21 (2010) 299-310

DOI: 10.1016/j.tetasy.2010.01.001

[38] D. S. McGuinness, A. J. Rucklidge, R. P. Tooze, A. M. Z. Slawin Organometallics 26 (2007) 2561-2569

DOI: 10.1021/om700740g

[39] D. S. McGuinness Chem. Rev. 111 (2011) 2321-2341

DOI: 10.1021/cr100217q

fig

Click here to access/download;Figures;Fig 10.png

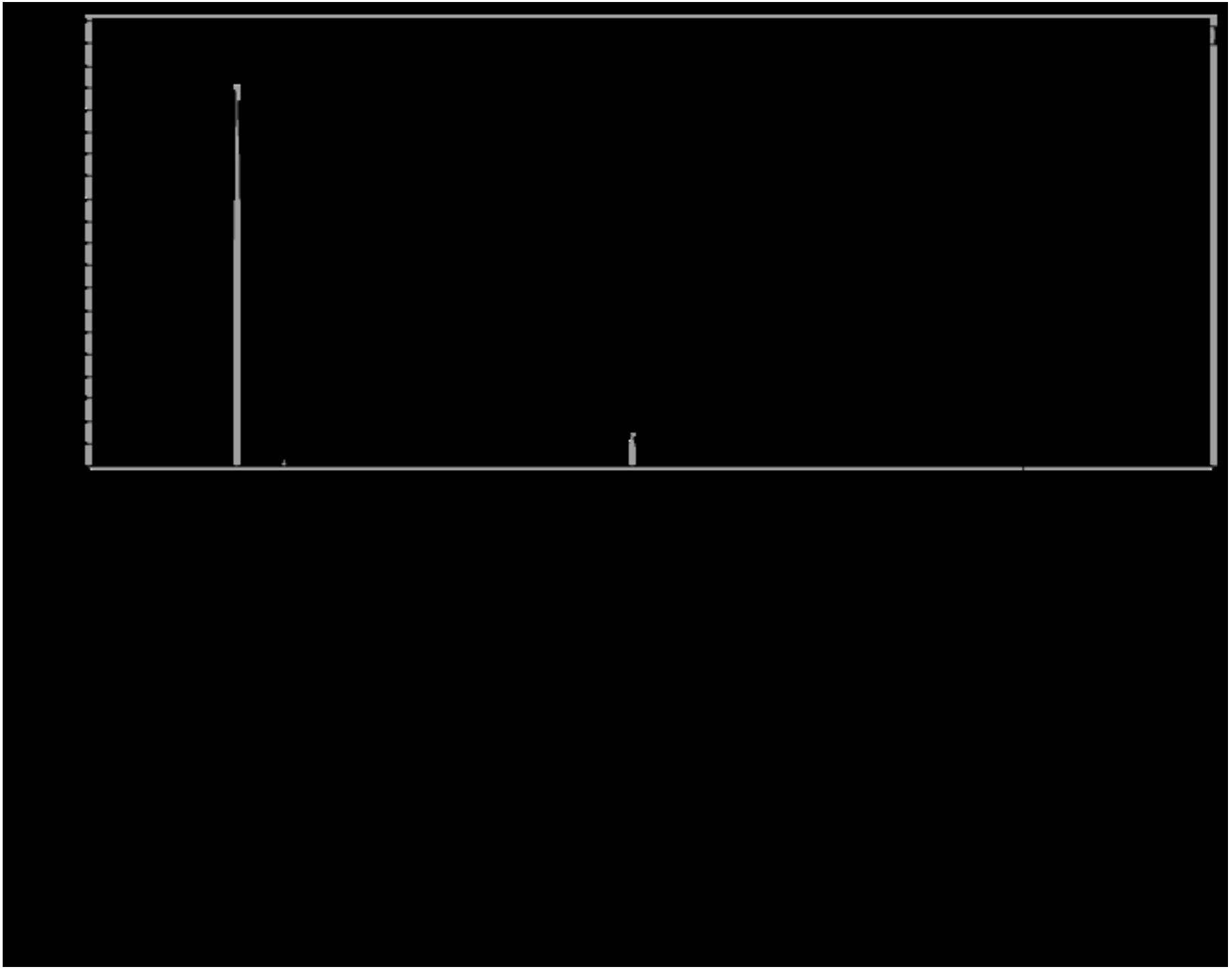

fig

Click here to access/download;Figures;Fig 1 left.png

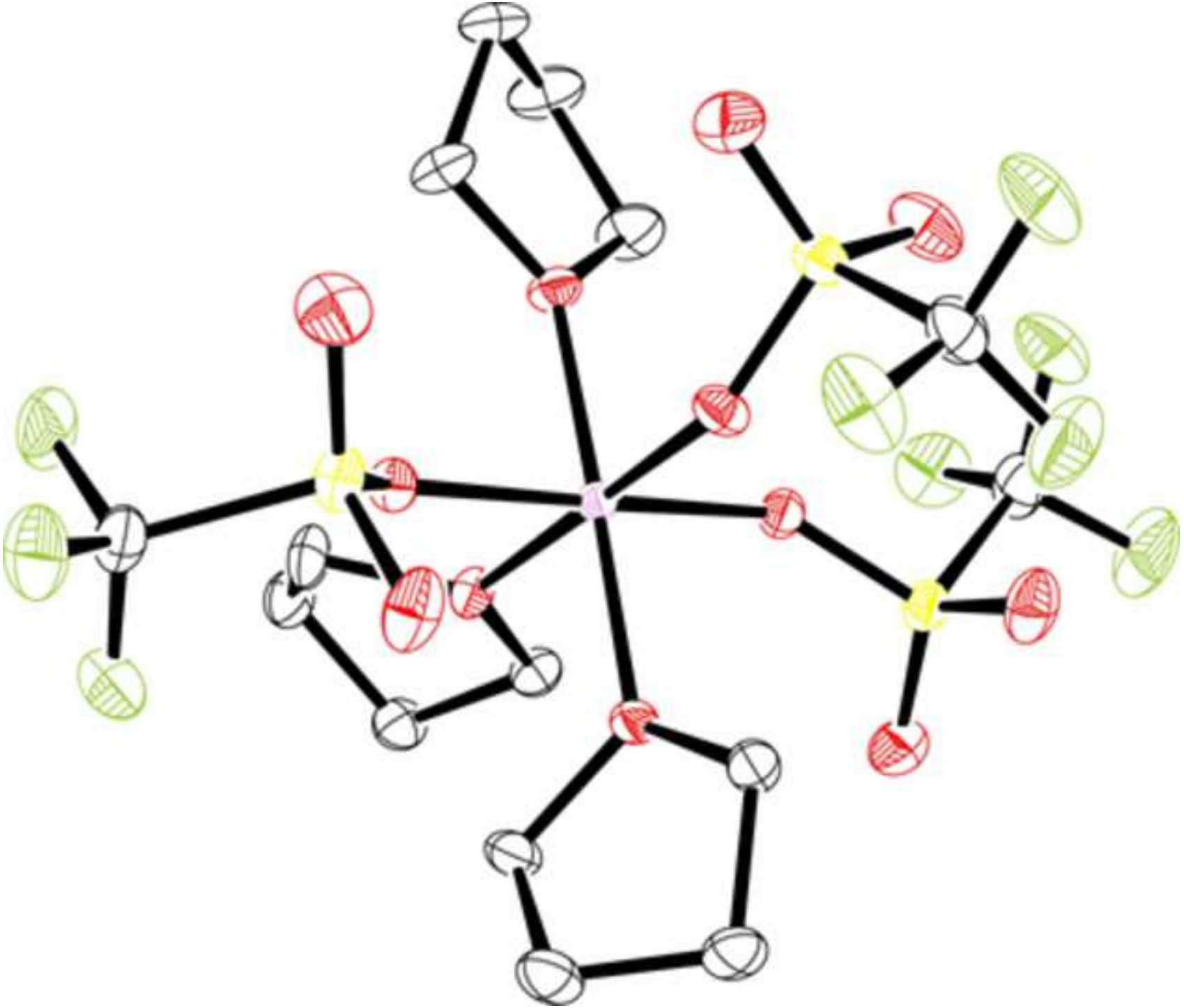

fig

Click here to access/download;Figures;Fig 2a.jpg

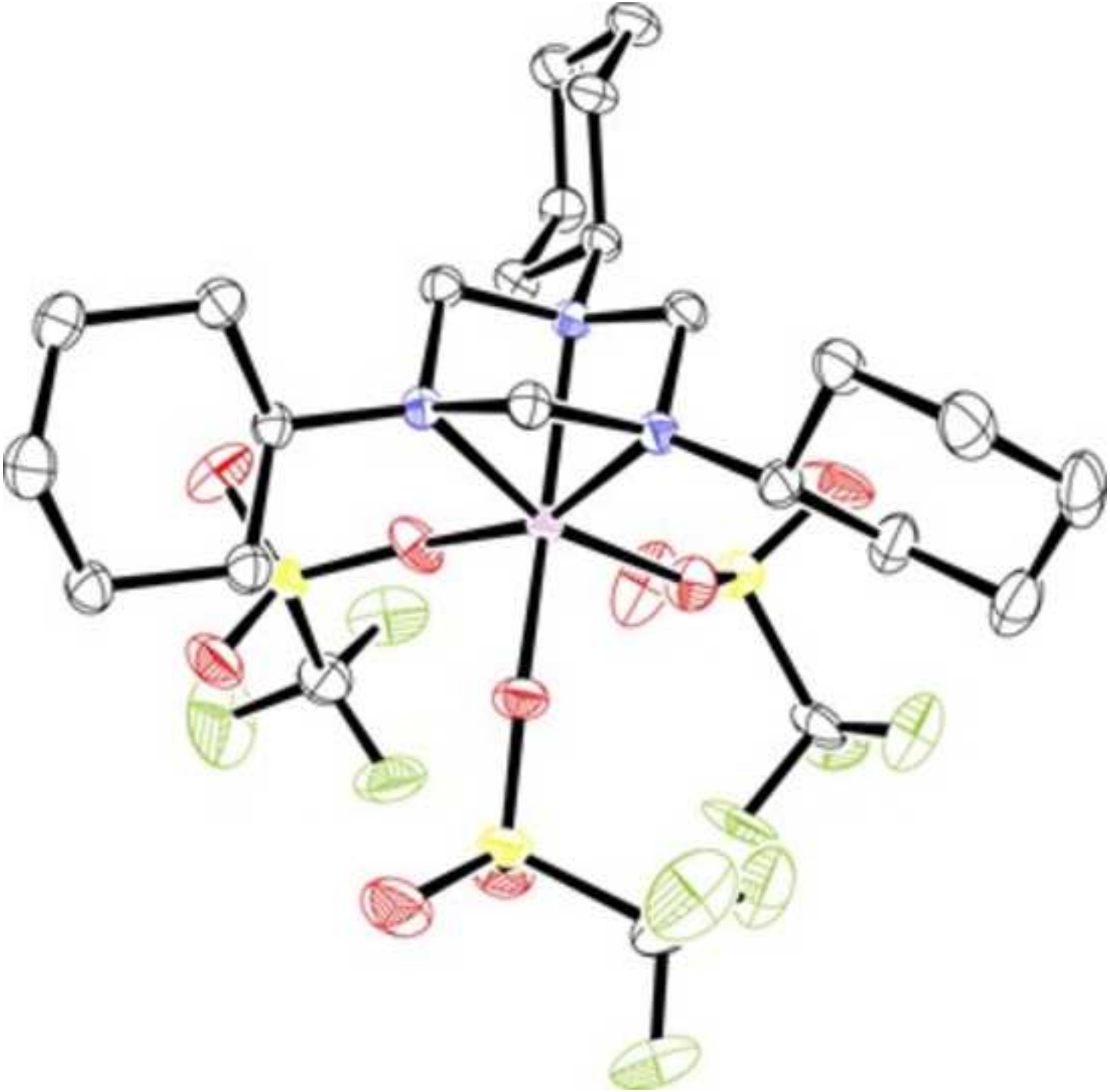

fig

Click here to access/download;Figures;Fig 2a.png

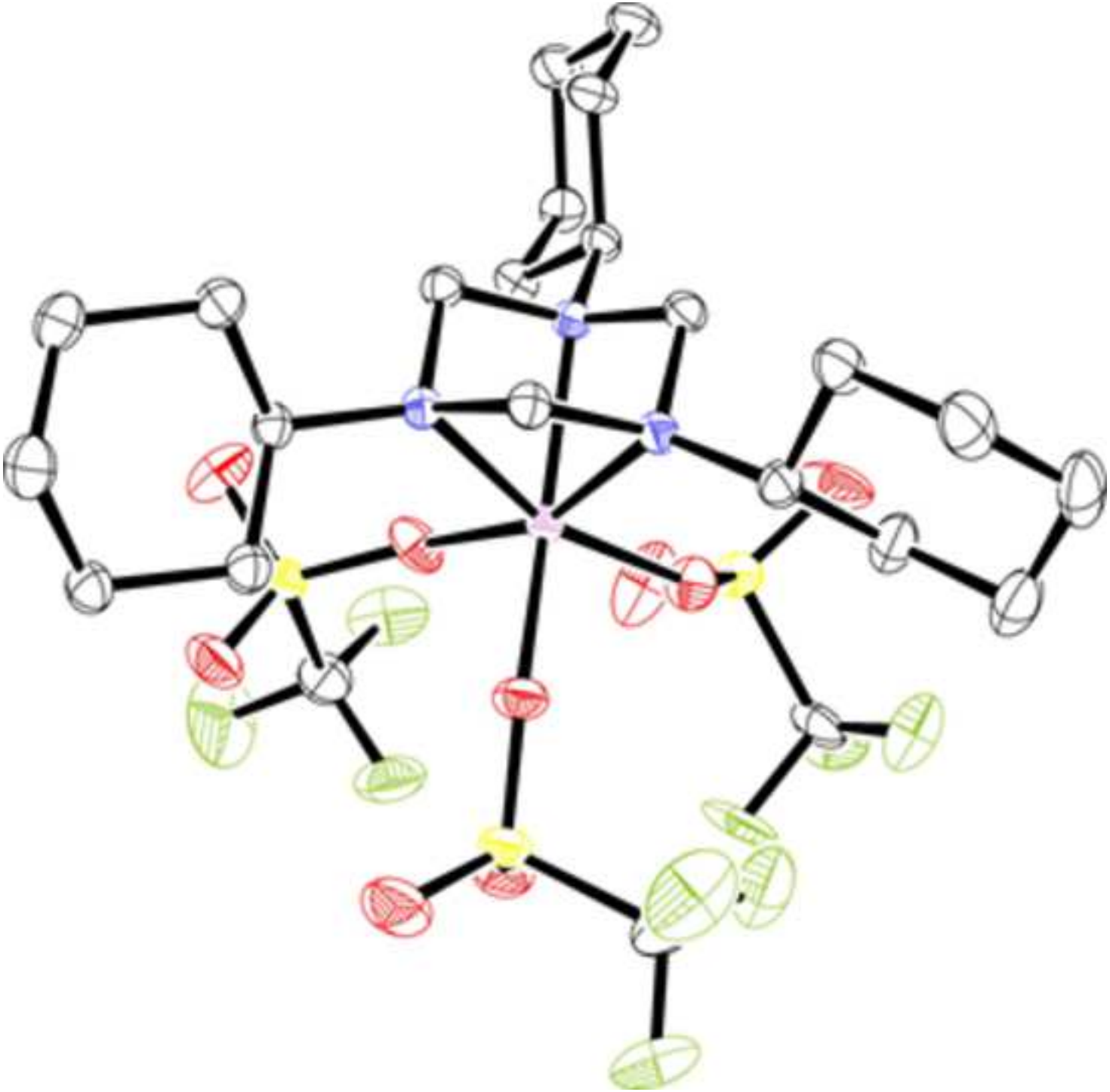

fig

Click here to access/download;Figures;Fig 2b.jpg

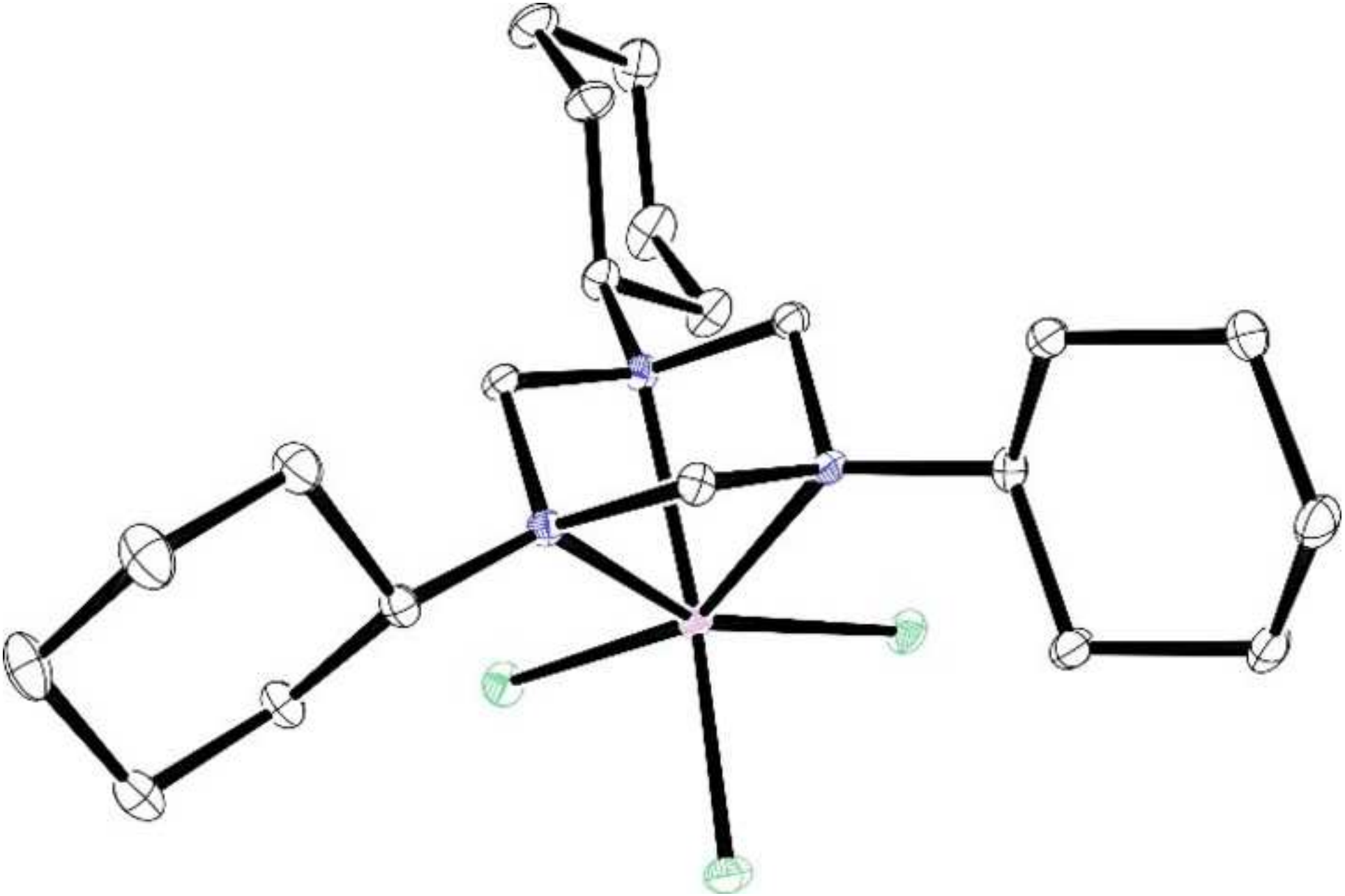

fig

Click here to access/download;Figures;Fig 2c.jpg

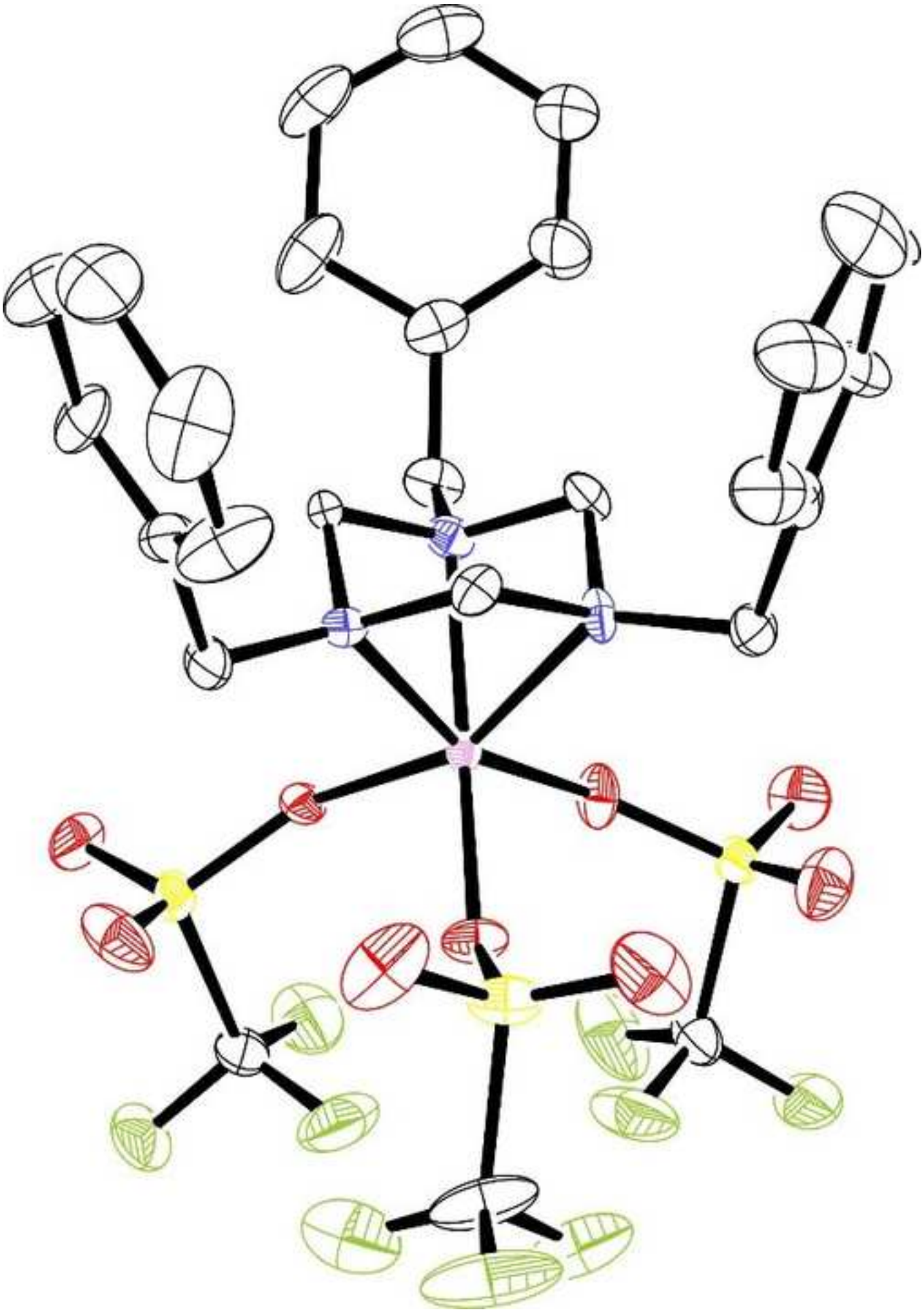

fig

Click here to access/download;Figures;Fig 2d.jpg

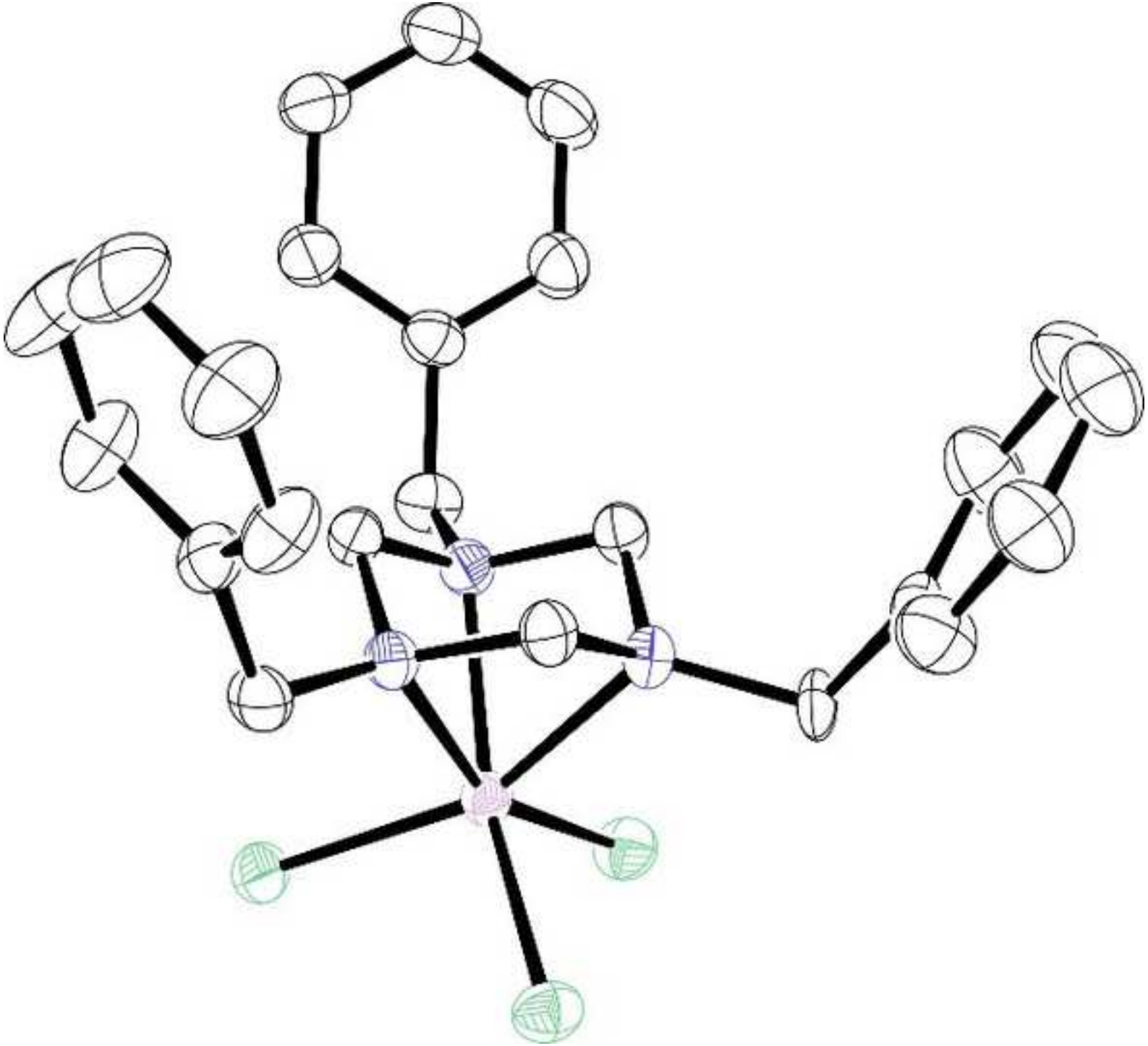

fig

Click here to access/download;Figures;Fig 3.tif

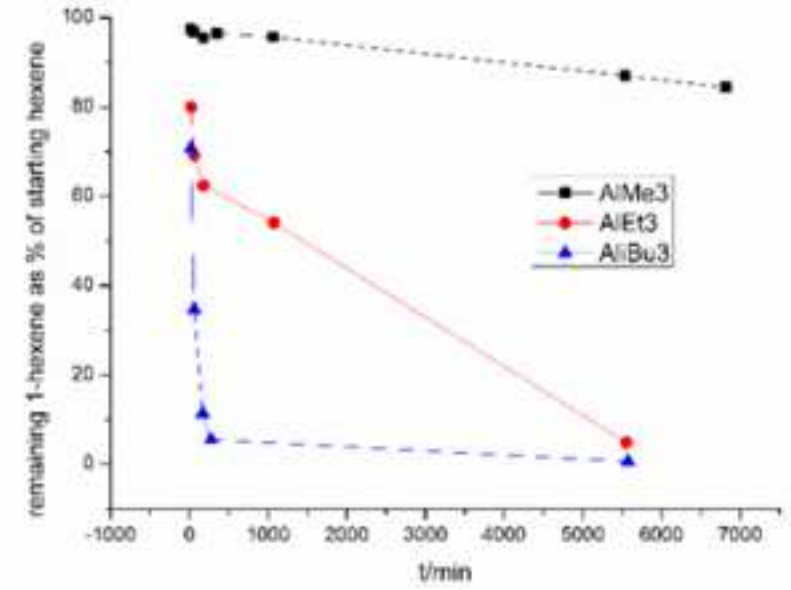

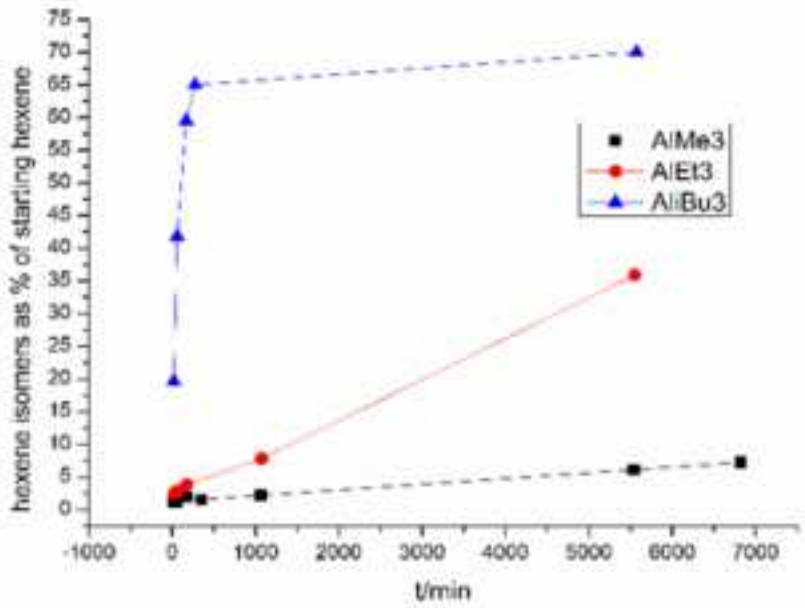

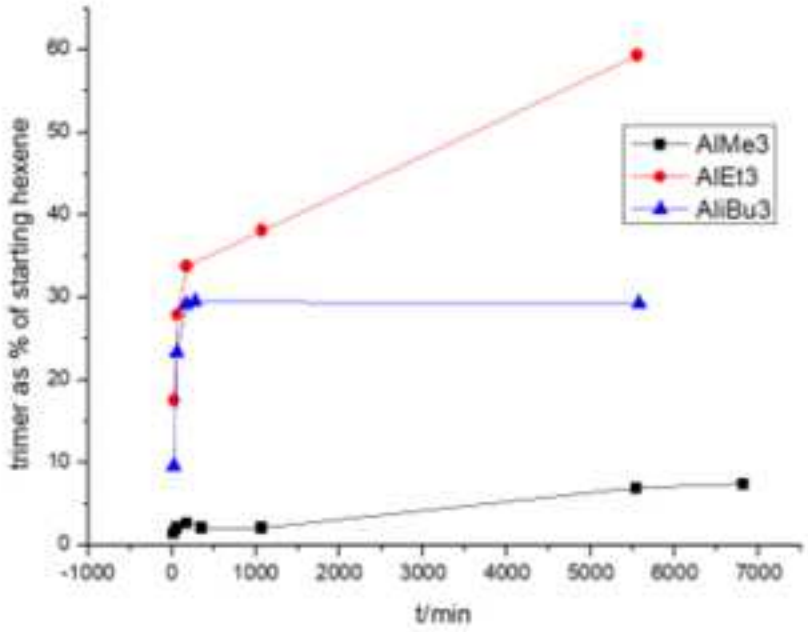

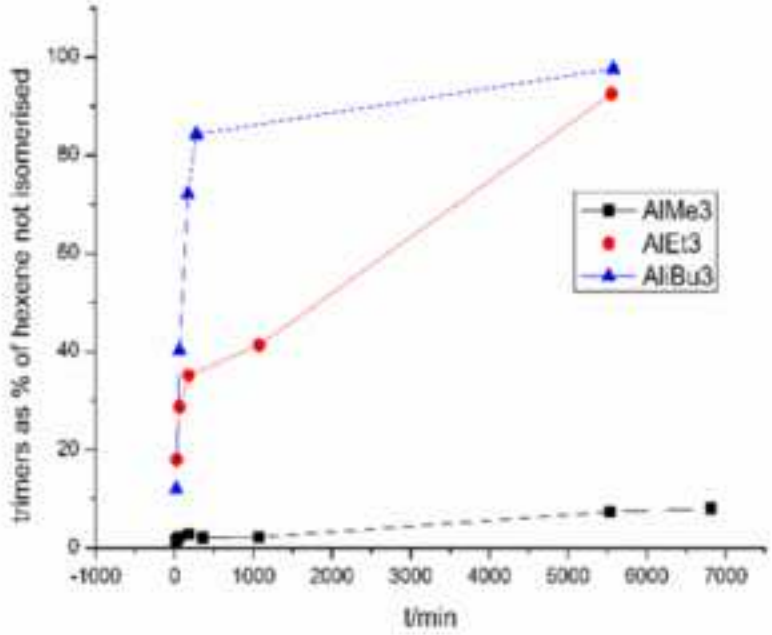

fig

Click here to access/download;Figures;Fig 4.tif

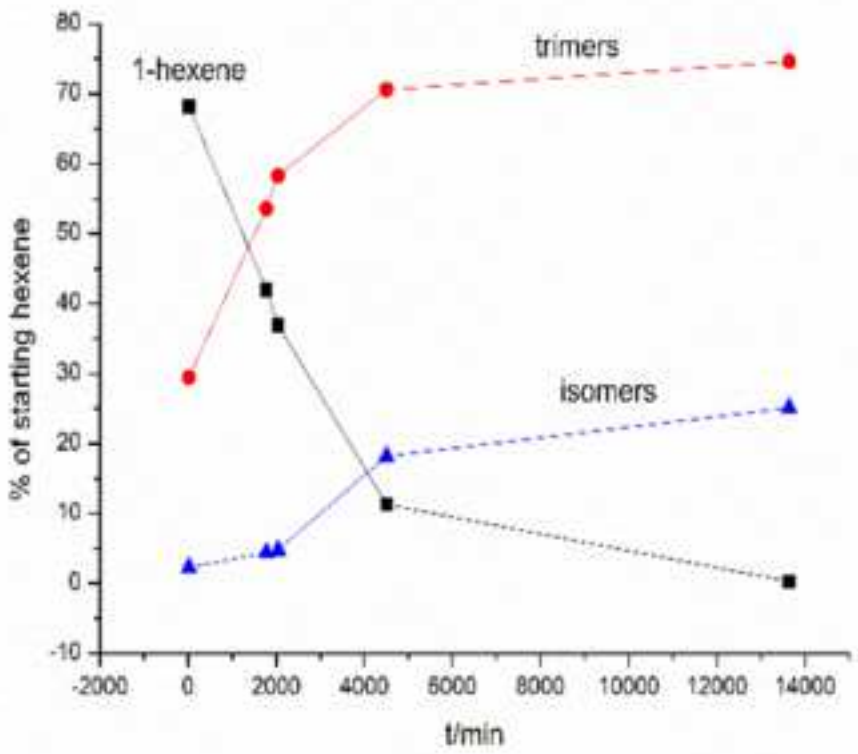

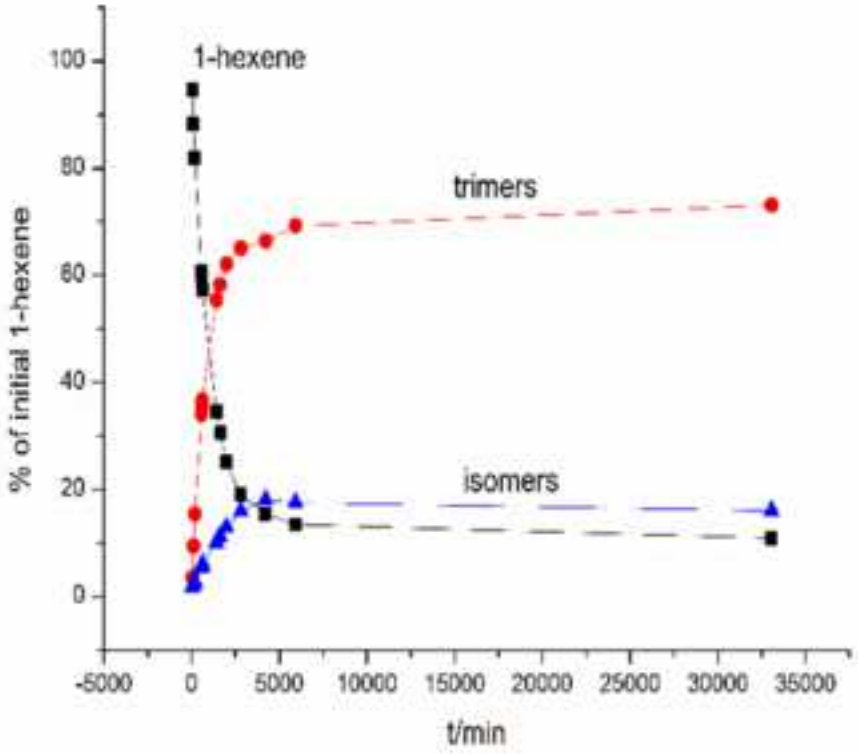

fig

Click here to access/download;Figures;Fig 5.png

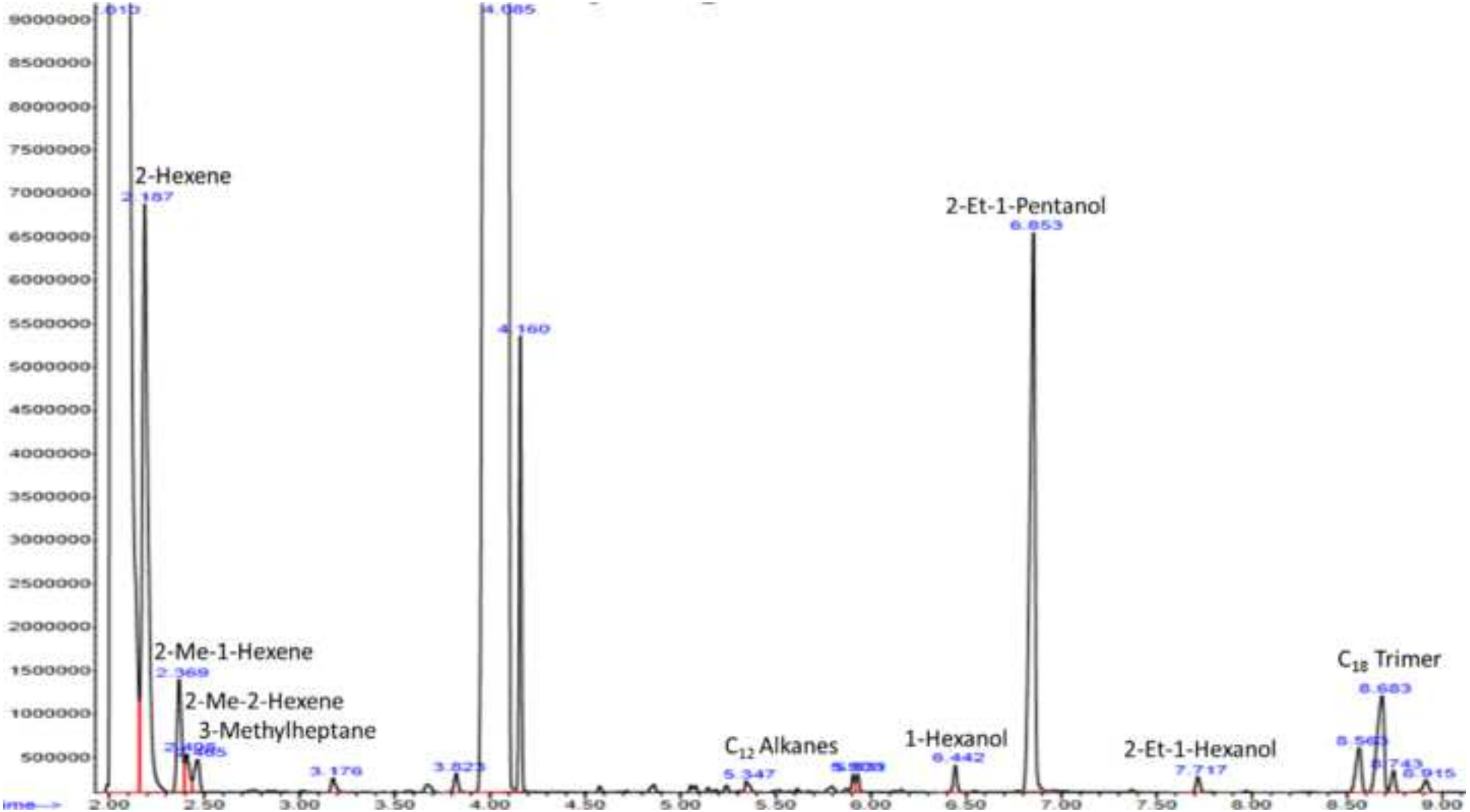

fig

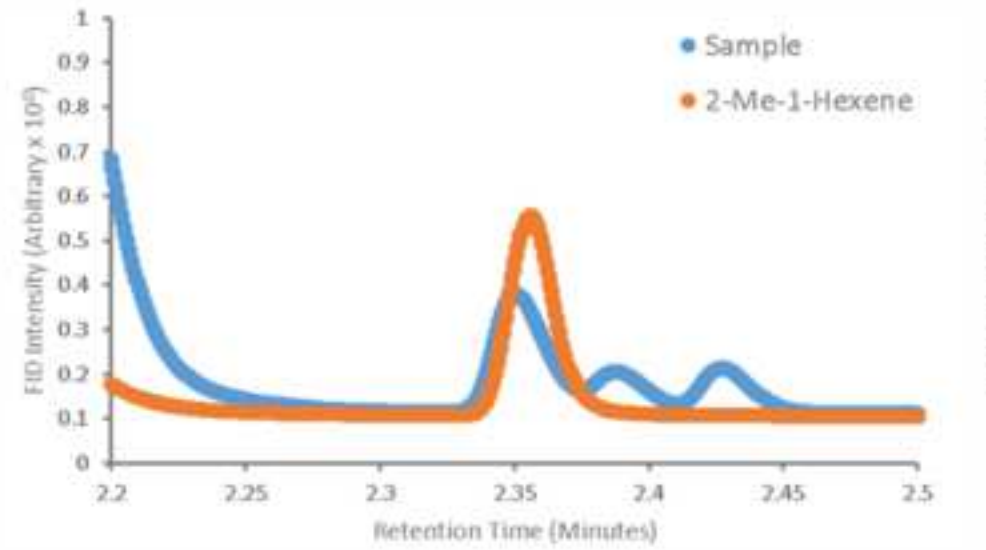

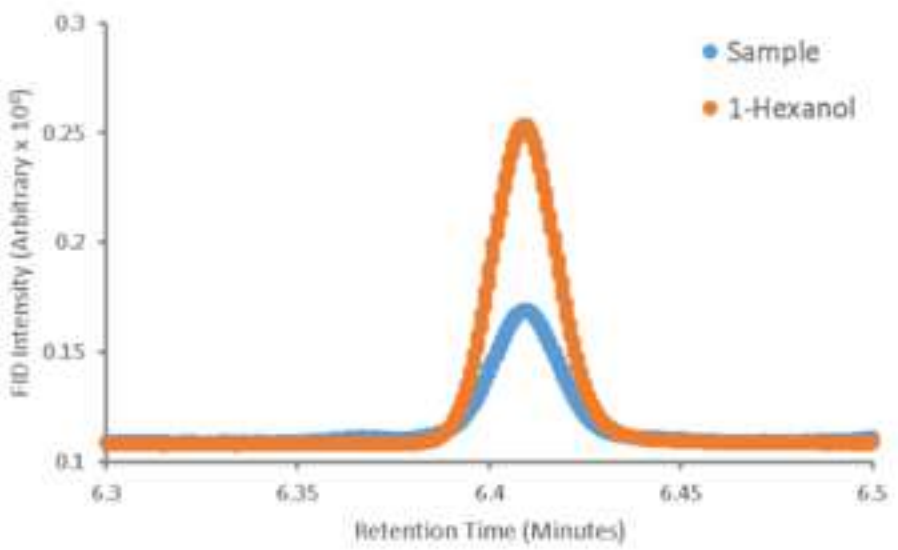

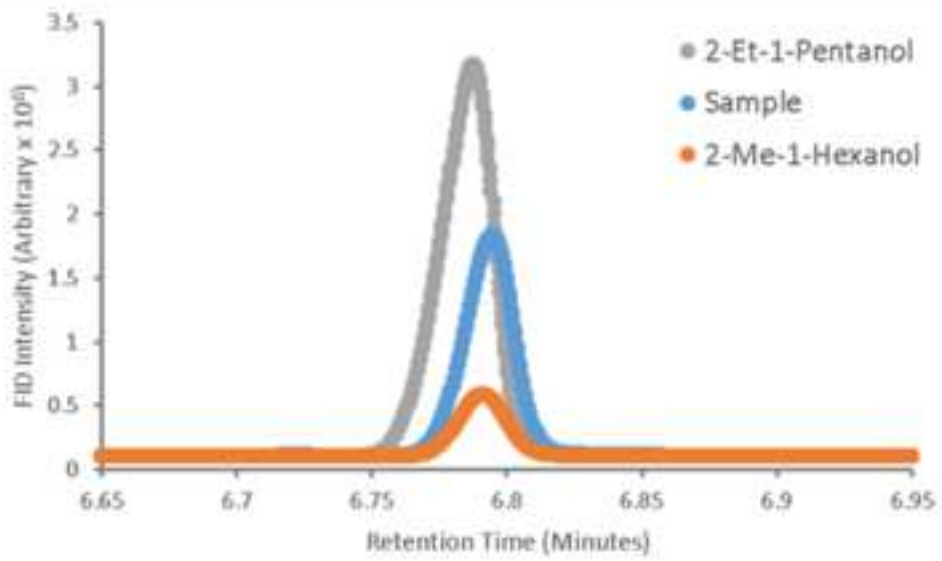

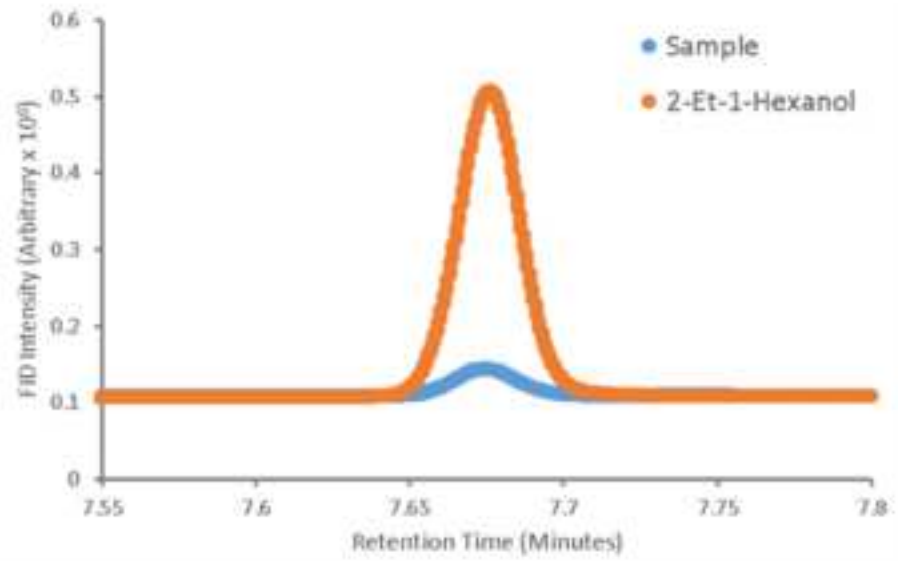

fig

Click here to access/download;Figures;Fig 7.jpg

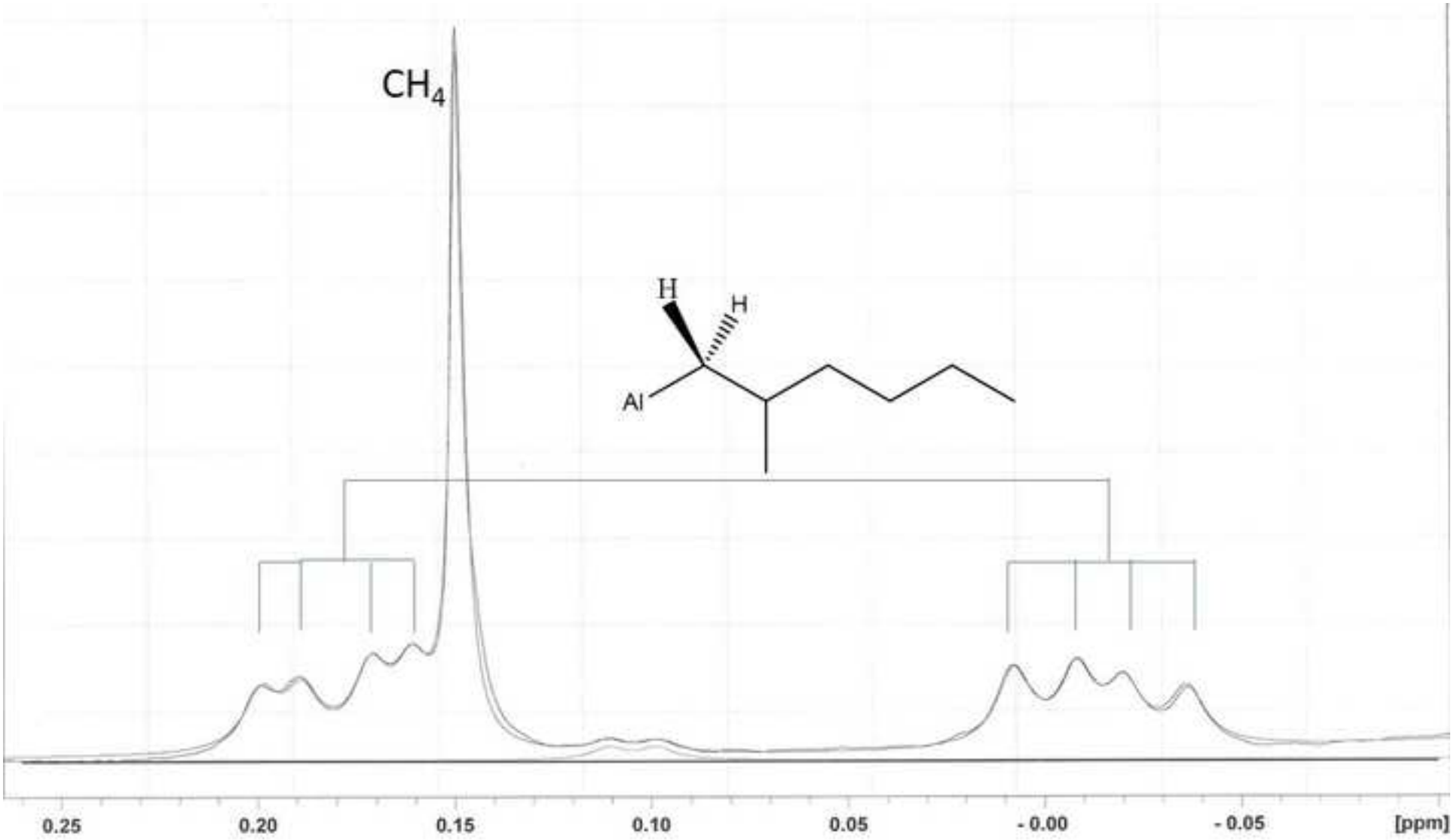

fig

Click here to access/download;Figures;Fig 8.jpg

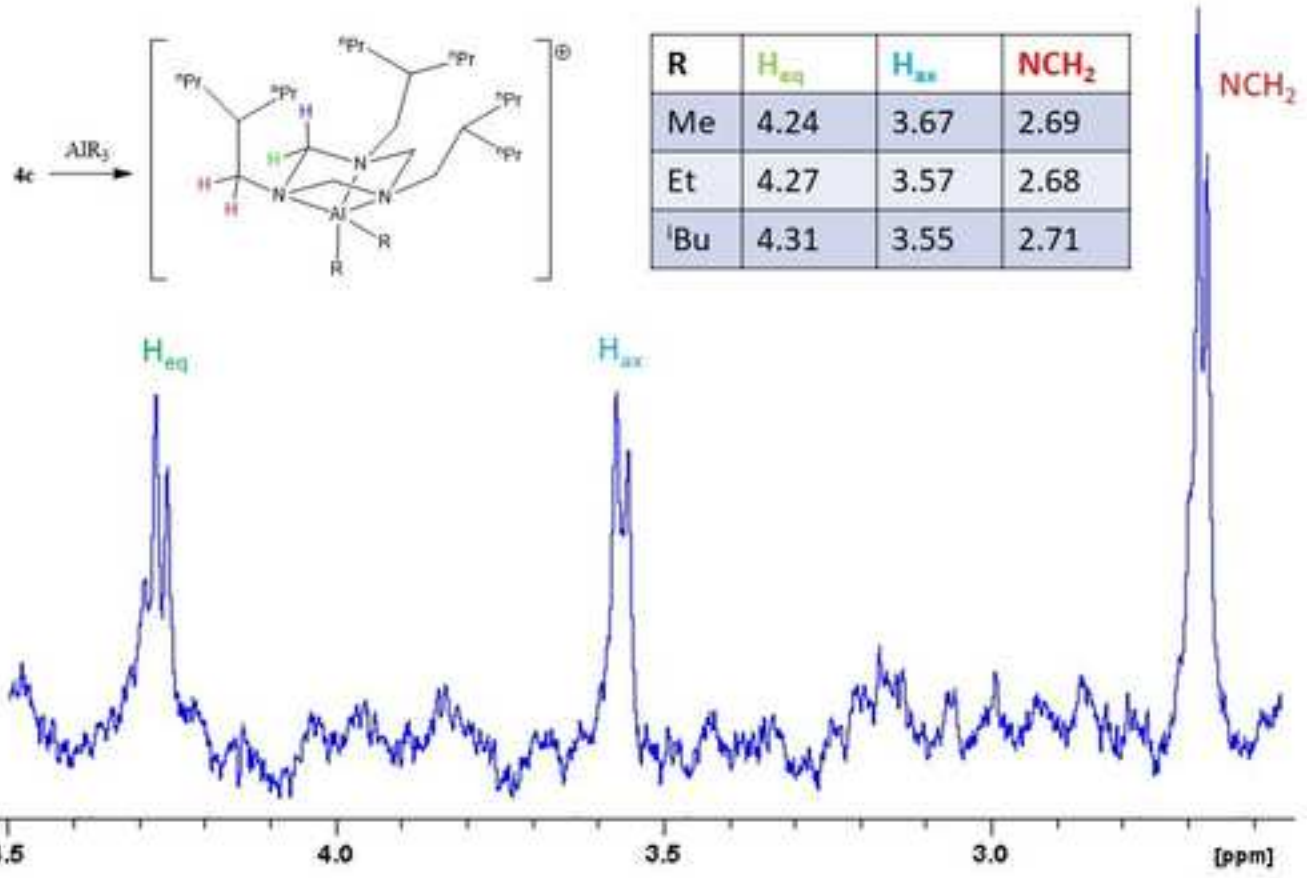

R	H_{eq}	H_{ax}	NCH_2
Me	4.24	3.67	2.69
Et	4.27	3.57	2.68
^{i}Bu	4.31	3.55	2.71

fig

Click here to access/download;Figures;Fig 9.png

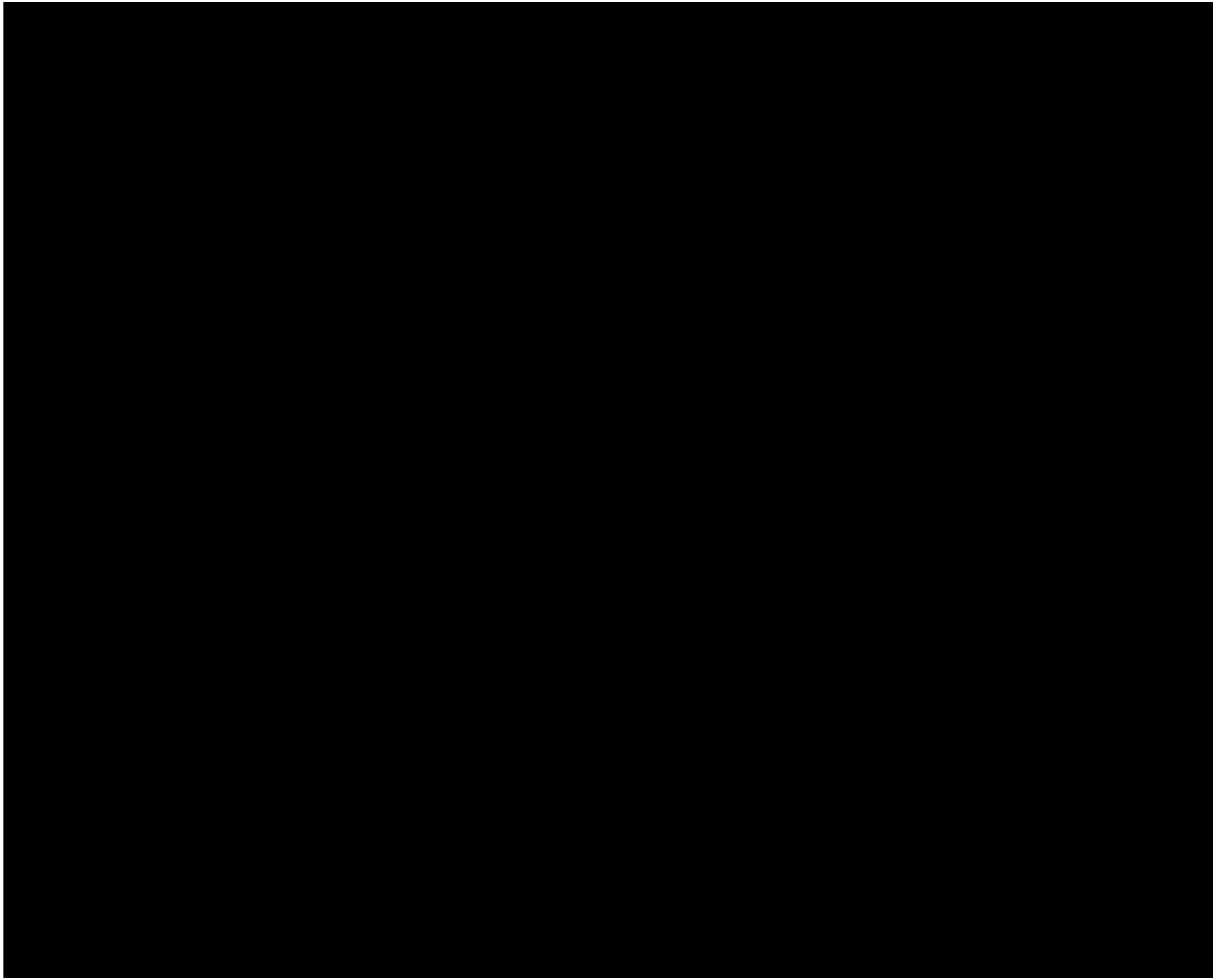

CIF (*if crystal structure is described)

Click here to access/download

CIF (*if crystal structure is described)

CrCl3(THF)3.cif

CIF (*if crystal structure is described)

Click here to access/download

CIF (*if crystal structure is described)

[Cr(H2O)6]3+ .cif

CheckCIF (*if crystal structure is described)

CheckCIF (*if crystal structure is described)

CheckCIF (*if crystal structure is described)

chart

chart

chart

graph

scheme

scheme

scheme

scheme

scheme

Declaration of interests

☒ The authors declare that they have no known competing financial interests or personal relationships that could have appeared to influence the work reported in this paper.

☐The authors declare the following financial interests/personal relationships which may be considered as potential competing interests:

CRediT author statement

Randolf D. Köhn: Conceptualization, Methodology, Investigation, Writing - Original Draft, Writing - Review & Editing, Supervision, Project administration; **Alexander G. N. Coxon**: Methodology, Investigation, Writing - Original Draft; **Samaphon Chunawat**: Investigation; **Callum Heron**: Investigation; **Shahram Mihan**: Resources, Supervision, Funding acquisition, Project administration; **Catherine L. Lyall**: Methodology, Resources, Writing - Review & Editing; **Shaun Reeksting**: Methodology, Resources; **Gabriele Kociok-Köhn**: Resources, Writing - Original Draft, Writing - Review & Editing